

**ISRO - NASA**  
**AVIRIS – NG Airborne Flights over India**  
**Science Plan Document**  
**for Hyperspectral Remote Sensing**

DRAFT

<b>CONTENTS</b>		
		<b>Page no.</b>
<b>1.0</b>	<b>INTRODUCTION AND BRIEF HISTORY</b>	<b>3</b>
<b>2.0</b>	<b>HYPERSPECTRAL APLICATIONS</b>	<b>4</b>
<b>2.1</b>	<b>GLOBAL SCENARIO</b>	<b>4</b>
<b>2.2</b>	<b>INDIAN SCENARIO AND CURRENT STATUS</b>	<b>5</b>
<b>3.0</b>	<b>NEED FOR HYPERSPECTRAL AIRBORNE/SPACE BORNE MISSION</b>	<b>8</b>
<b>4.0</b>	<b>MAJOR SCIENCE GOALS OF THE HYPERSPECTRAL MISSION (Themes, proposed sites, methodology, expected outcome)</b>	<b>13</b>
<b>5.0</b>	<b>CALIBRATION OF AIRCRAFT AND SATELLITE SENSORS</b>	<b>59</b>
	<b>REFERENCES</b>	<b>61</b>

## 1.0 INTRODUCTION AND BRIEF HISTORY

Imaging spectroscopy is of growing interest as a new approach to *Earth Remote Sensing*. With the advent of hyperspectral remote sensors, both airborne and space-borne, along with the high storage capacity of the fast computing systems and advanced software to store and process the hyperspectral data, it is now possible to detect and quantify various earth resource materials (Goetz, 2009). The original definition for imaging spectrometry proposed by the author and others (Goetz et al., 1985) was given as “the acquisition of images in hundreds of contiguous, registered, spectral bands such that for each pixel a radiance spectrum can be derived.” Hyperspectral sensors or imaging spectrometers collect unique data that are both a set of spatially contiguous spectra and spectrally contiguous images (Goetz *et al.* 1985). One of the earliest applications of hyperspectral remote sensing identified was geological mapping and its commercial role in mineral exploration.

The development of terrestrial imaging spectroscopy, as documented by Staenz, 2009, started in the late seventies by NASA’s Jet Propulsion Laboratory (JPL) and a government of Canada/private partnership (Department of Fisheries and Ocean/Moniteq) leading to the Airborne Imaging Spectrometer (AIS; Vane and Goetz, 1988) in the U.S.A. and the Fluorescence Line Imager (FLI; Gower et al., 1987) in Canada with first data acquisitions in 1983 and 1984, respectively. These activities led in 1987 to the first visible and near-infrared (VNIR) and short-wave infrared (SWIR) sensor, JPL’s Airborne Visible/Infrared Imaging Spectrometer (AVIRIS; Green et al., 1998; Vane et al., 1993) and in 1988 to the first commercial instrument, Itres’ Compact Airborne Spectrographic Imager (*casi*; Anger et al., 1990). Many more airborne systems have been developed since that time (e.g., Buckingham, 2008; Birk and McCord, 1994).

The first successfully launched civilian hyperspectral satellite sensor, NASA’s Hyperion on EO-1, has been in orbit since 2000 (Pearlman, 2003). A year later, the Compact High Resolution Imaging Spectrometer (CHRIS) on board ESA’s Project for On-Board Autonomy (PROBA) platform was launched (Barnsley et al., 2004). Both systems are still operating today, providing imagery in the VNIR (CHRIS) and VNIR/SWIR (Hyperion). With the current launches of ISRO’s VNIR HyperSpectral Imager (HySI) on board the Indian Microsatellite 1 (IMS-1) and the Chinese VNIR HJ-1A satellite sensor in 2008, new opportunities will arise for the use of hyperspectral data in various application areas due to the larger ground sampling distance (GSD)  $\leq 100$  m) combined with a larger swath width ( $\geq 50$  km) of these sensors (Goetz, 2009; Staenz, 2009).

Data handling and correction of sensor artefacts dominated software development in the early phases of imaging spectroscopy, followed by an intense period of algorithm development (AVIRIS, 2007). Innovative procedures, such as atmospheric correction and spectral linear unmixing, were developed (Staenz and Williams, 1997; Neville et al. 2008). These procedures together with the capability to handle hyperspectral data were incorporated into several hyperspectral image analysis systems by government and academic institutions and, ultimately, resulted in the release of the first commercial system, ENVI, in 1994 (Boardman

et al., 2006). With the availability of ENVI, the development of applications increased significantly, making imaging spectroscopy an important tool in areas such as climate change, resource management, and environmental monitoring and assessment as, for example, shown in the AVIRIS Workshop proceedings (AVIRIS, 2007). Additional hyperspectral image analysis systems have emerged, such as the hyperspectral packages in ERDAS Imagine and in PCI Geomatica (Goetz, 2009; Staenz, 2009).

## **2.0 HYPERSPECTRAL APPLICATIONS**

### **2.1 GLOBAL SCENARIO**

The term “hyperspectral imaging” was first coined by Goetz et al. (1985) in a paper discussing the early results of the technique of imaging spectrometry. Hyperspectral imaging has enabled applications in a wide variety of Earth studies (Goetz, 2009). The prime motivation for the development of imaging spectrometry was mineralogical mapping of surface soils and outcrops (Abrams et al., 1977; Goetz et al., 1985). The reflectance spectra of minerals are rich in electronic as well as overtone and combination vibrational features that characterize surfaces that are relatively vegetation-free (Clark et al., 1990). Only approximately 30% of the land surface is relatively devoid of vegetation and the remaining 70% is covered by vegetation to the extent that the substrate is rendered inaccessible to remote sensing identification (Siegal and Goetz, 1977). However, the vegetation cover, its type, health, vigor and expression of environmental conditions including the substrate are the subject of many ongoing studies (Goetz, 2009).

Wessman et al. (1988) identified tree species for the first time based on nitrogen and lignin content in the foliage. They used statistical regression techniques also known to spectroscopists as chemometrics (Mark, 1989) and built a prediction model based on known occurrences of broadleaf and evergreen species on Blackhawk Island, WI. As follow-on to the HIRIS project, NASA funded the Accelerated Canopy Chemistry Program in which chemometrics techniques were used successfully on AVIRIS data acquired over the Harvard Forest, MA (Aber & Martin, 1995; Martin and Aber, 1997) (Source: Goetz, 2009). Other diverse studies of species and canopy health, water content as well as relative abundances of photosynthetic (PV) and non-photosynthetic (NPV) vegetation in a pixel can be found in papers by Gamon et al. (1992, 1993), Ustin et al. (1992, 1998), Roberts et al. (1993, 1998), and Asner and Lobell (2000) (Source: Goetz, 2009).

Studies of the coastal zone are better served by hyperspectral imaging, which makes it possible to unmix the bottom and several in-column constituents (Carder et al., 1993; Lee et al., 1994). Hyperspectral imaging is equally applicable to the solid water phase which makes it possible to study the properties of ice and snow, in particular grain size (Nolin & Dozier, 1993; Painter et al., 1998). Environmental studies using hyperspectral imaging are yielding results that would be impossible to obtain or would be prohibitive in cost or time spent with standard techniques. One example that has been documented to have saved millions of dollars

is in the cleanup of the Leadville, CO Superfund Site in which AVIRIS images combined with field spectral measurements identified the waste piles with the greatest potential for leaching heavy metals into streams and groundwater (Swayze et al., 2000). Asbestiform minerals have also been identified in situ from AVIRIS data (Swayze et al., 2005). Maps of expansive soils, important in construction engineering, can also be identified in AVIRIS images (Chabrilat et al., 2002) (Source: Goetz, 2009).

## ***2.2 INDIAN SCENARIO AND CURRENT STATUS***

Indian researchers are actively engaged in making use of the potential of hyperspectral data since late 1990's and early 2000's in various fields of applications such as agriculture, precision farming, pest and disease, forestry, coastal applications and geological and mineral exploration and spectral library related activities.

Land applications include vegetation studies (species identification, plant stress, productivity, leaf water content, and canopy chemistry), soil science (type mapping and fertility status), geology (mineral identification and mapping) and hydrology (snow grain size, liquid/solid water differentiation). Lake, river and ocean applications include biochemical studies (phytoplankton mapping, activity), water quality (particulate and sediment mapping) and bathymetry. Atmospheric applications include parameter measurement (water vapor, ozone, and aerosols) and cloud characteristics (optical thickness, cirrus detection, particle size). All these work were carried out in collaboration with various state and national agencies relevant in respective fields and the study sites also were spread over various parts over India. Few studies also been carried out for wetland ecosystem and the results showed that different wetland plots have similar spectra curves while they still possible to be distinguished in some visible and NIR in hyperspectral data. Many applications with hyperspectral data were carried out for mineral exploration, and snow studies in the Himalayan region. These studies showed the capability of hyperspectral data for identifying and quantifying minerals and rocks as well as mapping the indicators for mineral exploration; and for studying the effect of contamination and grain size variability on snow. These studies also derived the optimum hyperspectral bands for these studies.

### ***Earth and Planetary Sciences Applications***

Geological mapping and mineral exploration are better manifested in spectral signatures and spatial distributions identifiable through remote sensing techniques. This helps in delineating exploration targets for metals and industrial minerals (Kruse 1988). Studies on laboratory spectroscopy (Hunt and Salisbury 1970, Clark *et al.* 1990) and data using remote imaging spectrometers (Kruse 1988, Kruse *et al.* 1990, Staenz and Williams 1997, Kruse *et al.* 2003, Neville *et al.* 2003) have well established its efficiency in mineral identification, quantification, mapping and exploration.

Detailed field based spectral measurements are being carried out at various places in India in order to characterize the spectral features of exposed mineral guides such as the Gossans mostly associated with poly-metallic sulphide deposits, hydrothermal alteration zones

associated with porphyry copper deposits, iron ores, bauxites and laterites spread over vast expanses of Deccan Traps, mapping of Uraniferous calcretes in the spectral range of 350-2500 nm (Bharti et al., 2012; Bharti and Ramakrishnan, 2014; Bhattacharya et al., 2012; Das and Bhattacharya, 2012; Guha et al., 2013; Kusuma et al., 2012; Ramakrishnan et al., 2013; Sanjeevi, 2008; Sanjeevi et al., 2012??). A spectral cataloguing of the rocks and minerals associated with the mineralogical provinces and Precambrian terrain of eastern and northern Gujarat has also been prepared (Das and Bhattacharya, 2012). Work is also being carried out at SAC on the spectral characterization of Martian analogues from the Deccan Volcanic Province of Kachchh, Gujarat and Rakhabdev Ultramafic Suites of Rajasthan (Bhattacharya et al., 2012; Jain et al., 2011, 2012). Jarosite, an iron-bearing hydrous sulphate and a key Martian mineral having astrobiological significance has been reported for the first time from the laterite profile developed over the Deccan basalts at Kachchh near Matanumadh village, Gujarat (Bhattacharya et al., 2012; Jain et al., 2011) and a systematic spectroscopic and geochemical studies are being carried out at the laterite section of Matanumadh. Moreover, Bhattacharya et al. (2013, 2014) reported the presence of a Al-rich phyllosilicate over Fe-Mg-smectite stratigraphy developed in the saprolite-laterite profile at Matanumadh, similar to those observed at Mawrth Vallis and Meridiani Planum regions on Mars indicating changes in the paleoclimatic and paleodrainage conditions in the Kachchh region owing to the tectonic disturbances that the area had undergone in the past and is currently undergoing.

India's airborne imaging spectrometers, namely, Airborne IMaging Spectrometer – 2 (AIMS-2) and Airbone HyperSpectral Imager (A-HySI) were flown over the Shivrajpur-Khandia region of Gujarat in order to map the open cast manganese mine at Shivrajpur and the nearby old workings. The spectra were compared with the field based spectra of manganese ores. In Space-based Imaging Spectroscopy Bhattacharya et al. (2012) has detected and mapped the presence of altered/clay minerals by utilizing the 2.0-2.4  $\mu\text{m}$  spectral range of EO-1 Hyperion over parts of Dongargarh, Chattisgarh in conjunction with *in situ* field-based spectral measurements.

Furthermore, Imaging spectrometers are one of the most important tools used for the remote compositional assessment of any planetary surface. SAC-ISRO is actively involved in analyzing the data from Chandrayaan-1 hyperspectral instruments for compositional and mineralogical characterization of the lunar surface (Bhattacharya et al., 2011, 2012, 2013; Kaur et al., 2013; Lal et al., 2012). One of the major Indian contributions to Chandrayaan-1 mission and overall lunar science include the discovery of magmatic water on the Moon for the first time based on remote orbital measurements associated with non-mare silicic volcanic constructs (Bhattacharya et al., 2013). Apart from that, Indian researchers are also involved in the discovery of a new mineral "Spinel" on the lunar surface based on remote measurements (Bhattacharya et al., 2012, 2013, 2014; Chauhan et al., 2014, 2015; Lal et al., 2011, 2012; Kaur and Chauhan, 2014; Kaur et al., 2012, 2013a, 2013b; Srivastava et al., 2013). Apart from Moon, Jain and Chauhan (2015) and Jain et al. (2014) has detected and mapped the presence of phyllosilicates and carbonates from the Capri Chasma region within the Valles Marineris area of Mars highlighting the past liquid water activity on Mars.

### ***Snow, Glacier and Cryospheric Research***

Field based spectroradiometer observations have been taken for varying properties of snow physical properties in the Beas basin along with collateral data. Snow reflects strongly in the visible region and decreases in the NIR and SWIR region. The effect of various atmospheric and meteorological conditions influences the snow properties and reflectance which has been studied using ground based instruments. Hyperion satellite data was used to retrieve the grain size in part of Himalayas. Singh et al. (2010, 2011) had studied the effects of soil and coal contamination and grain size on the snow reflectance. Continuous field-based spectral measurements have been conducted in the Himalayan cryosphere which are useful to develop new algorithms for retrieving various snow and glacier parameters (Negi et al., 2015).

### ***Agricultural Applications***

Agriculture forms important field for hyperspectral studies owing to diversity in the crop growing conditions and management practices. These complexities get compounded to variety of factors such as soil, water, management and crop varieties etc. In the field of crop science major works carried out are - Pulse crop discrimination, Crop stage discrimination and analysis of angular effect, Crop biophysical parameter retrieval, Tea crop discrimination studies and crop residue studies. These studies identified important narrow bands required for pulse crop discrimination, important view angle and hyperspectral indices for crop stage discrimination, identified hyperspectral indices for LAI and plant nitrogen estimation, Optimum bands for tea crop identification, optimum bands as well as important indices for crop residue studies. Crop disease discrimination in mustard crop was carried out by Bhattacharya and Chattopadhyay (2013) using EO-1 Hyperion data over Bharatpur region in Rajasthan

For soil science, hyperspectral data were used for Soil fertility parameter retrieval and mapping, Soil variability mapping and fertility zonation, Estimation of Soil parameters like bulk density, EC, nitrogen, phosphorus etc. These studies concluded that several soil properties, namely, surface condition, particle size, organic matter, soil colour, moisture content, iron and iron oxide content and mineralogy can be mapped through imaging spectroscopy and that hyperspectral data can be effectively used for generating soil variability and fertility zonation.

Crop stage discrimination using IMS-1 HySI has also been carried out. Works have carried out to develop Spectral signature bank and prototype spectral library of vegetation; develop Software for Reflectance Spectra Analysis and PROSAIL Model Inversion.

### ***Forestry Applications***

In the field of forestry major works carried out at SAC are - Forest species discrimination and biochemical parameter retrieval, Mangrove species identification and Discrimination of Mangrove ecosystem components and associated features. The results confirmed that there

are significant differences in pigment levels, and optical properties for leaves of tropical dry forests. Different variables of leaves of forest species like phenology, age etc can be discriminated based on their spectral reflectance properties. These studies also found out the best classifier for forest species discrimination. Discrimination of forest species and narrow band indices correlation with biochemical components were studied. The components of hyperspectral pre processing and classification algorithms were also evaluated for forest species.

### ***Wetland Ecosystem***

The deterioration of the ecological status of continental waters (dams, lakes, lagoons) has become an urgent and growing problem in the last years. In this regard, evaluation of hyperspectral data for wetland ecosystem was done for Chilika Lagoon, Orissa

### ***Biological Oceanographic Applications***

Exhaustive studies using under water radiometer has been done in coastal and open ocean waters of Arabia sea and Bay of Bengal for Phytoplankton function types and various species identification. Also, studies were conducted for water quality evaluation, IOPs and eutrophication studies of inland water bodies using underwater radiometer. Coastal water studies for geophysical parameter retrieval were extensively carried out in Arabian sea.

## **3.0 NEED FOR HYPERSPECTRAL AIRBORNE/SPACE BORNE MISSION**

Hyperspectral imager (HSI) can detect the individual absorption features, since all the materials are bound by chemical bonds, thus they can be identified by their spectral characteristics more accurately as compared to broad band multi-spectral imagers. Spaceborne hyperspectral data have three potential advantages over space borne multispectral sensors- they can provide an enhanced level of information for atmospheric correction to derive surface reflectance; they can provide access to detailed spectral indices; they can be used to integrate the hyperspectral data consistently to synthetic bands equivalent to any other broad band sensors or to bands of yet to be developed instruments. Hyperspectral remote sensing technologies have allowed the development of an increasing number of spectral bands and, consequently, an improved capability for gaining a greater understanding of the fundamental processes that govern changes in the biophysical/biochemical properties of vegetation. Hence in the past many activities involving hyperspectral data (from ground based, airborne and space borne) were successfully planned and carried out at the Space Applications Centre, Ahmedabad. Applications are being pursued in all areas of Earth science including land, water and atmospheric topics.

In mineral exploration, presence of hydrothermal alteration zones associated with granite batholiths, oxidized gossans with goethite/limonite/hematite capping are often act as important indicators for possible existence of sub-surface ore bodies. Hyperspectral remote sensors or imaging spectrometers can efficiently characterize these indicators based on diagnostic absorption features of hydrothermal alteration minerals and gossan assemblages,



primarily arising due to the electronic charge transition of  $\text{Fe}^{2+}/\text{Fe}^{3+}$  and/or overtones and combination tones of hydroxyl and/or water and/or carbonates/sulphates in the crystal lattice of hydrothermal and gossan mineral assemblages, which are otherwise impossible to detect and characterize using broad-band or multi-spectral instruments as the bands in multi-spectral sensors are widely separated in spectral space and width of the individual spectral channels are so broad that these type of instruments cannot detect the diagnostic absorption features of minerals and rocks.

Precise analysis of Band Center, Band Strength, and Band shape and asymmetry factor, Integrated Band Depth (IBD) /Band Area and Band Curvature can help in discriminating amongst the dominant gossan mineral species and also one can study the relative abundances of the species present and generate fraction map. Spatial resolution of the space-borne hyperspectral instruments are not good enough to study the mineral prognostic zones and the exposure sizes and vegetation cover play major roles in determining the discrimination capability of the space-borne hyperspectral instruments as coarser resolution will have more spectral mixing of endmember species. Therefore, there is a need to have airborne hyperspectral campaigns over mineral prognostic zones, areas of geological importance and volcanoes in a targeted mode to have better spatial resolution, which, in turn, will help in detecting more and more pure endmember mineral species and rock types thereby producing a better mineralogical and lithological map. There is a need to have various mineral and rock indices to detect and map guides for mineral exploration, to study the lava chemistry and pyroclastic deposits associated with active and dormant volcanoes and also to spectrally characterize the sites of geological importance such as paleo-subduction zones, exposed layered intrusive complexes, suture zones and ophiolites etc.

### **AVIRIS-NG AND JPL**

Airborne Imaging Spectrometer (AIS) of JPL, NASA is considered as the first ever airborne hyperspectral instrument that was flown successfully for the first time over Cuprite, Nevada in August, 1983. The mineral identification success, and in particular the discovery of buddingtonite, an ammonium feldspar, became part of a Public Broadcasting System (PBS) documentary while the gold pathfinder mineral question was still open, led to a greater interest within NASA to pursue further sensor development (Goetz, 2009). In 1984, JPL proposed an imaging spectrometer program that would encompass an advanced airborne sensor, the airborne visible/infrared imaging spectrometer (AVIRIS), and two orbiting sensors, the shuttle imaging spectrometer experiment (SISEX) and a free-flyer, the high resolution imaging spectrometer (HIRIS) (Goetz, 2009). AVIRIS development was begun in 1984 and the imager first flew aboard a NASA ER-2 aircraft at 20 km altitude in 1987. Since then it has gone through major upgrades as technology changed in detectors, electronics and computing. AVIRIS is arguably the finest, best calibrated, airborne imaging sensor ever flown, which is the result of the dedication of the instrument leaders and their teams at JPL, Gregg Vane (Vane et al.,1993) and Robert O. Green (Green et al.,1998) and the continuing support of Diane Wickland of NASA Headquarters (Goetz, 2009).

In the late 1980's, several commercial hyperspectral imagers entered the market. The first was DAIS from Geophysical Environmental Research of Millbrook, NY (Richter, 1996). In 1989 ITRES Corporation, Alberta, Canada introduced CASI, an imaging spectrometer covering the visible and near-infrared region to 900 nm utilizing a 2-d silicon CCD array (Dekker et al., 1992). In 1994, the Naval Research Lab sensor HYDICE was completed (Basedow & Zalewski, 1995). This sensor was designed around a prism dispersion concept and a single, hybrid HgCdTe 2-d array to cover the 400–2500 nm spectral region. Although HYDICE began as a dual-use program, it soon reverted to an all DOD program. Other commercial sensors in this wavelength region are available. The one most like AVIRIS is the Australian sensor HyMap from the HyVista Corporation, which markets a full-range (400–2500 nm) hyperspectral imaging service on a global basis. Airborne Prism Experiment (APEX) is another recent imaging spectrometer, collecting information in the spectral range of 380-2500 nm and is developed by a Swiss-Belgian consortium for the European remote sensing community on behalf of ESA. It is also intended as a support for calibration and validation and a simulator for future spaceborne hyperspectral imagers (APEX Science Center - RSL – University of Zurich. contact: michael [schaepman@geo.uzh.ch](mailto:schaepman@geo.uzh.ch); APEX Operation Center – VITO contact: [koen.meuleman@vito.be](mailto:koen.meuleman@vito.be)).

The advanced AVIRIS instrument, i.e., AVIRIS-NG uses most advanced state-of the-art detector array and grating for dispersion of light. Most importantly, the blazing and grooving technique employed in the grating of AVIRIS-NG could successfully maintain the spectral as well as spatial uniformity, thus completely removing the SMILE and KEYSTONE effects that used to be the integral part of all the earlier hyperspectral instruments.

An example AVIRIS imaging cube is shown in Figure 1. A set of research and applications examples are included in this document from investigation pursued with AVIRIS in North America. For every example related AVIRIS data sets may be download so that early data processing preparation for the airborne campaign with AVIRIS-NG may begin. AVIRIS-NG is a higher performance, more recent instrument and the instrument planned for the airborne campaign.

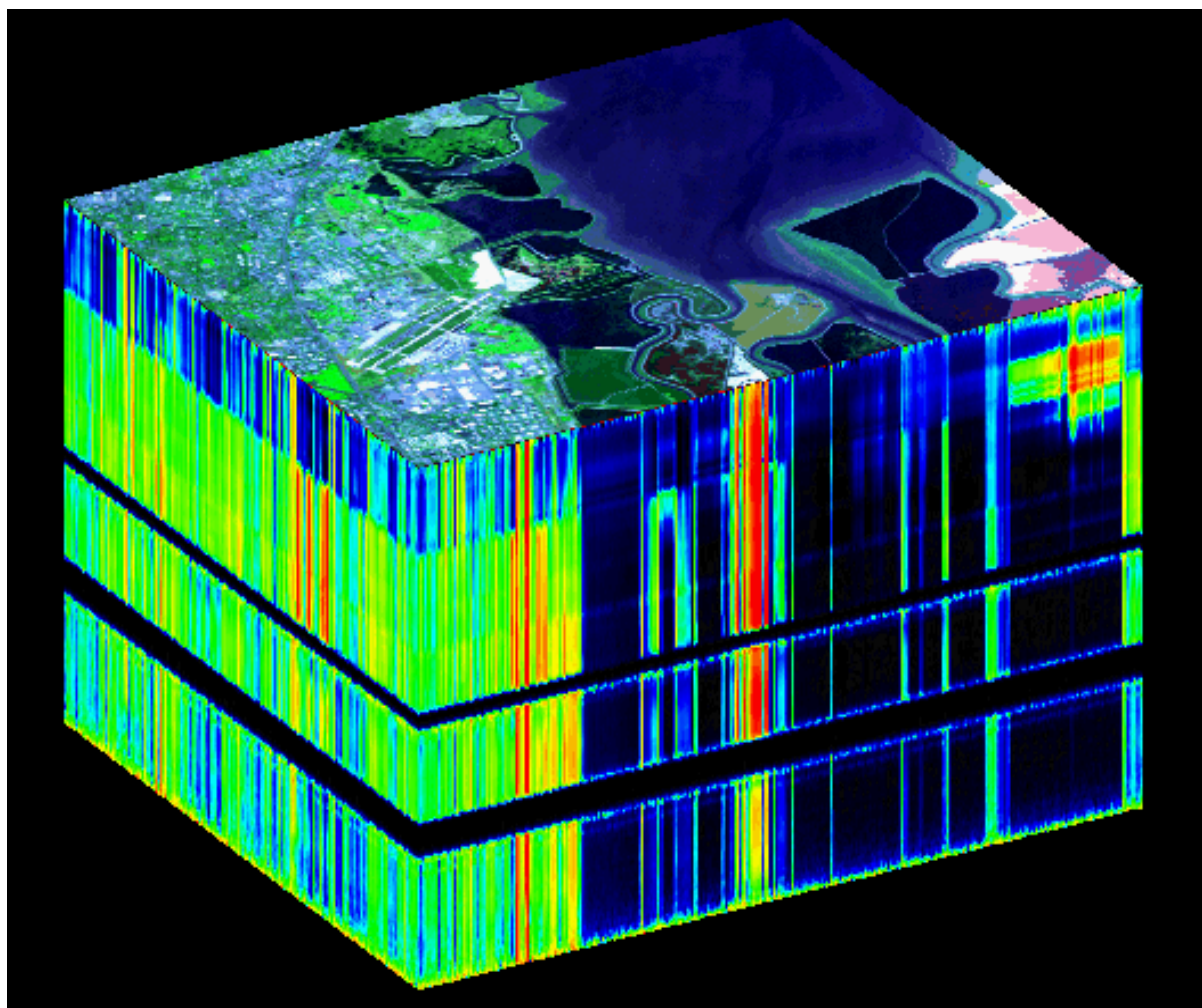


Figure 1. Example JPL AVIRIS image cube with a spectrum acquired for each point in the image for spectroscopic analysis (R. Green).

This effort will bring together important talents of both NASA and ISRO to address unique and urgent Earth remote measurement set of science and application research for the 21st Century and can be executed under existing umbrella agreement with NASA and ISRO. The collaboration will provide opportunity for joint development of science models, algorithms, atmospheric corrections and can open up new avenues. Considering JPL's capability and experience, this will lead to sharing of scientific knowledge within the appropriate governmental constraints. Airborne campaigns will provide the required precursor ground truth data and science and application research demonstrations for present and future ISRO space imaging spectrometer missions.

The airborne campaign can be targeted post monsoons during October to December 2015. However a contingency mission can be planned till the period of February. The mission aims at science and applications capability building and uses ISRO aircraft. The target areas for imaging spectroscopy science, application investigation and demonstration will be on Indian Territory after due clearance. The targeted applications will address:

- Agriculture and Ecosystems
- Mineral resource Mapping and Geochemistry



- Coastal Ocean
- Rivers and Water Quality
- Urban and Cities
- Snow and Ice Hydrology
- Cloud and atmosphere
- CAL-VAL

The science and applications program will be jointly developed with NASA-JPL and involve collaboration with NASA science and applications research. This document contains the proposal for the science plan that has been worked out. Various areas have been identified covering all the targeted application and a draft imaging targets is as shown in the figure 2

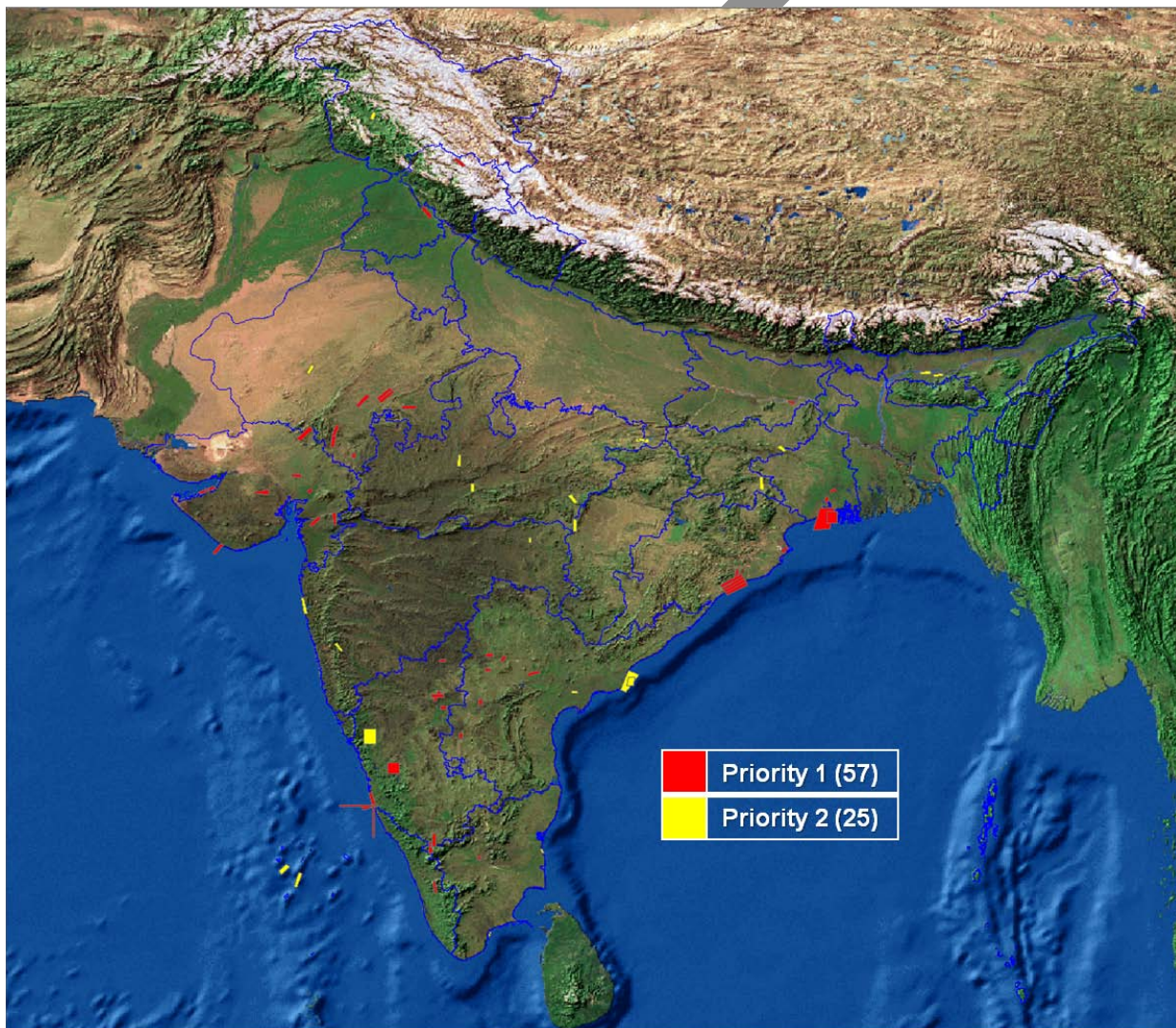


Figure 2 Proposed Imaging areas over India with AVIRIS - NG

## 4.0 MAJOR SCIENCE GOALS OF THE HYPERSPECTRAL MISSION

The major science goals of the hyperspectral mission include studies pertaining to agriculture and soils, wetlands ecosystems, mangrove ecosystems, coral reef ecosystems, forest ecosystem, mineral exploration, snow and glacier, lake ice, urban and cities, coastal/oceanographic applications, CRZ studies, atmosphere and calibration of aircraft and satellite sensors.

Details are mentioned as below:

### 4.1 AGRICULTURE AND ECOSYSTEM STUDIES

#### AGRICULTURE AND SOILS

**Goal: Crop assessment, discrimination, pests and disease assessment and parameter retrieval**

Imaging spectroscopy data consists of hundreds or thousands of narrow-wavebands along the electromagnetic spectrum; it is important to have narrow bands that are contiguous for strict definition of spectral data; and not so much the number of bands alone. Space imaging spectrometer data have at least three potential advantages over space multispectral sensors-1. They can provide an enhanced level of information for atmospheric correction to derive surface reflectance; 2. They can provide access to detailed spectral indices; 3. they can be used to integrate the spectral data consistently to synthetic bands equivalent to any other multispectral broad-band sensor or to bands of yet to be developed instruments. Imaging spectroscopy remote measurement technologies have allowed the development of an increasing number of spectral bands and, consequently, an improved capability for gaining a greater understanding of the fundamental processes that govern changes in the biophysical/biochemical properties of vegetation.

Imaging spectroscopy has demonstrated applicability for the characterization of diversity and richness of ecosystems. Imaging spectrometer data is fast emerging to provide practical solutions in characterizing, quantifying, modeling, and mapping natural vegetation and agricultural crops. The advantages of space systems are their capability to acquire data: (a) continuously, (b) consistently, and (c) over the entire globe. The subtle information of vegetation is manifested as function of structural and/or biochemical constituents in absorption/reflectance (3).

The spectroscopic signature of vegetation can be used to measure species type, vegetation, function and health. Figure 4 show an AVIRIS imaging spectrometer data set and the corresponding species map using a multiple end member spectral mixture analysis algorithm. In preparation for the airborne campaign, AVIRIS data sets from North America relevant to natural ecosystems of both calibrated radiance and reflectance may be downloaded from the website [http://aviris.jpl.nasa.gov/alt\\_locator/](http://aviris.jpl.nasa.gov/alt_locator/).

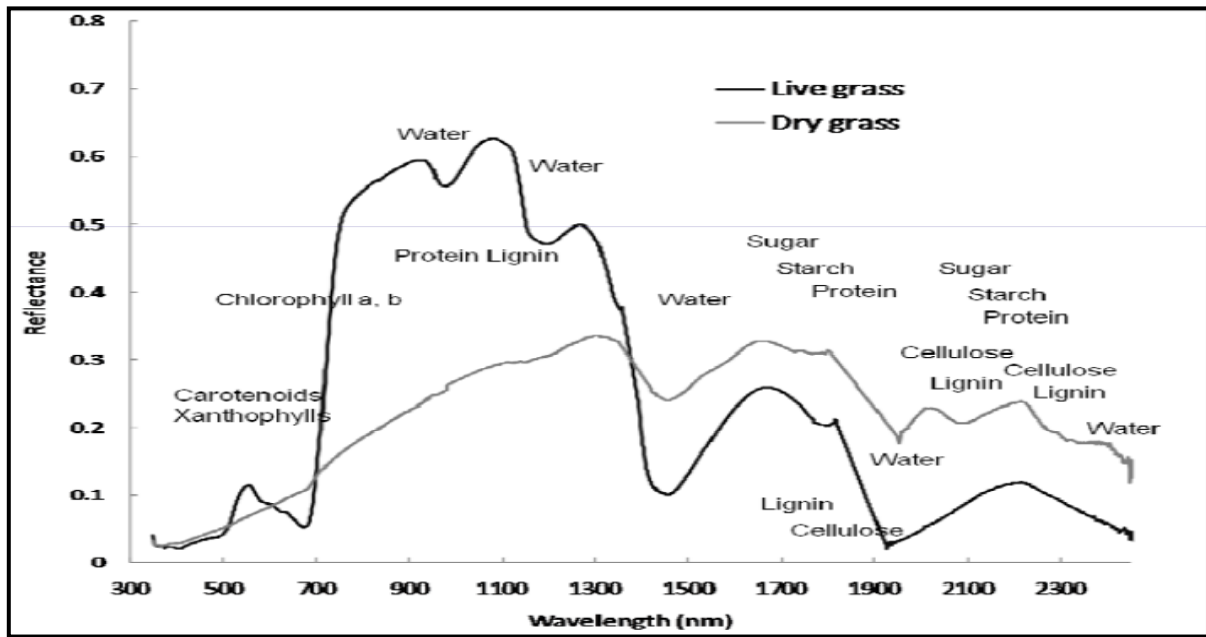


Figure 3 Absorption features associated with plant biochemical constituents for live and dry grass (Adapted from- Tenkabail, 2011) Anthocyanin (Anth), Chlorophyll (Chl), Water and Ligno-cellulose absorptions.

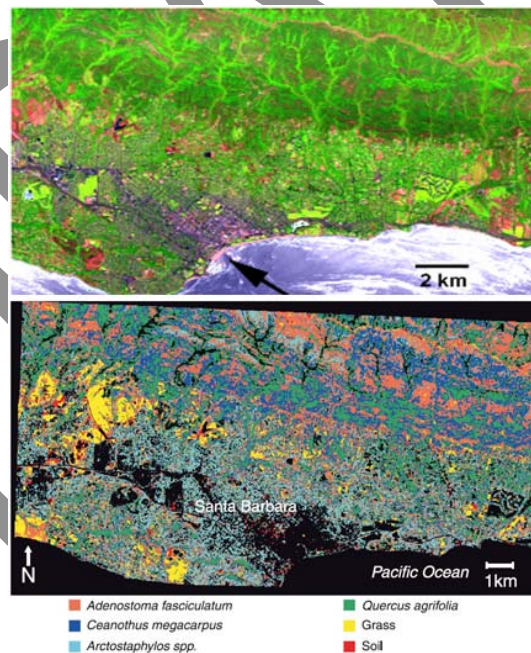


Figure 4. Example high level species map from AVIRIS imaging spectrometer measurement in the Santa Barbara area, California (D. Roberts, UCSB).

Unique features and strengths of spectral vegetation indices (SVIs) (Table 1) is useful for variety of applications in understanding the subtle information which otherwise is not amenable in broad band. These are useful in elimination of redundant bands, physically meaningful interpretation is feasible (e.g., Photochemical reflective index as proxy for light use efficiency). Significant improvement over broadband indices were observed using SVIs

e.g., reducing saturation of broad-bands, providing greater sensitivity (e.g., an index involving NIR reflective maxima @ 900 nm and red absorption maxima @680 nm). New indices not sampled by broad-bands e.g., water-based indices (e.g., involving 970 nm or 1240 nm along with a non-absorption band). The SVIs are of biophysical, biochemical, pigment, water, lignin and cellulose, and physiology based nature.

Table 1 Spectral Vegetation Indices

Index	Computation	Reference
Structural indices		
NDVI (Normalized Difference Vegetation Index)	$(\rho_n - \rho_r) / (\rho_n + \rho_r)$	Rouse et al. (1973)
SR (Simple Ratio)	$\rho_n / \rho_r$	Birth and McVey (1968)
SAVI (Soil Adjusted Vegetation Index)	$(\rho_n - \rho_r) (1+L) / (\rho_n + \rho_r + L)$ , L=0.5	Huete (1988)
MSAVI2 (Modified SAVI)	$\rho_n + 0.5 - ((\rho_n + 0.5)^2 - 2(\rho_n - \rho_r))^{0.5}$	Qi et al. (1994)
OSAVI (Optimized SAVI)	$(1+0.16) (\rho_{800} - \rho_{670}) / (\rho_{800} + \rho_{670} + 0.16)$	Rondeaux et al. (1996)
MSR (Modified SR)	$MSR = ((R_{800} - R_{670}) - 1) / ((R_{800} + R_{670}) / 0.5 + 1)$	Chen (1996)
RDVI (Renormalized Difference Vegetation Index)	$RDVI = (R_{800} - R_{670}) / (R_{800} + R_{670})^{0.5}$	Roujean and Breon (1995)
EVI (Enhanced Vegetation Index)	$EVI = 2.5 * ((R_n - R_r) / (R_n + 6R_r - 7.5R_{blue} + 1))$	Huete et al. (1997)
ARVI (Atmospherically Resistant Vegetation Index)	$ARVI = (R_n - (2R_r - R_{blue})) / (R_{nir} + (2R_{red} - R_{blue}))$	Kaufman and Tanre (1996)
Greenness/pigment related indices		



MCARI (Modified CARI)	$MCARI = [(R700 - R670) - 0.2(R700 - R550)] (R700/R670)$	Daughtry et al. (2000)
TCARI (Transformed CARI)	$TCARI = 3 [(R700 - R670) - 0.2(R700 - R550)] (R700/R670)$	Haboudane et al. (2002)
TVI (Triangular vegetation index)	$TVI = 0.5 [120 (R750 - R550) - 200 (R670 - R550)]$	Broge and Leblanc (2000)
SIPI (Structural insensitive pigment index)	$SIPI = (R800 - R445)/(R800 + R680)$	Penuelas et al. (1995)
NPCI (Normalized Pigment Chlorophyll Index)	$NPCI = (R680 - R430) / (R680 + R430)$	Penuelas et al. (1995)
PRI (Photochemical Reflectance Index)	$PRI = (\rho_{531} - \rho_{570}) / (\rho_{531} + \rho_{570})$	Penuelas et al. (1994)
RGR (Red Green Ratio Index)	$RGR = R_g / R_{red}$	Gamon and Surfus (1999)
Red Edge Normalized Difference Vegetation Index	$RedNDVI = (R750 - R705) / (R750 + R705)$	Gitelson and Merzylak (1994), Sims and Gamon (2002)
mSR (Modified Red Edge Simple Ratio Index)	$mSR = (R750 - R445) / (R705 - R445)$	Sims and Gamon (2002)
Modified Red Edge Normalized Difference Vegetation Index	$(R750 - R705) / (R750 + R705 - 2R445)$	Sims and Gamon (2002), Datt et al. (1999)
Vogelmann Red Edge Index 1	$VOG1 = R740 / R720$	Vogelmann et al. (1993)
Vogelmann Red Edge Index 2	$VOG2 = (R734 - R747) / (R715 - R726)$	Vogelmann et al. (1993)
Vogelmann Red Edge Index 3	$VOG3 = (R734 - R747) / (R715 - R720)$	Vogelmann et al. (1993)
Red Edge Position Index	Between 690 and 740nm	Curran et al. (1995)
CRI1 (Carotenoid Reflectance Index 1)	$CRI1 = (1/R510 - 1/R550)$	Gitelson et al. (2002)
CRI2 (Carotenoid Reflectance Index 2)	$CRI2 = (1/R510 - 1/R700)$	Gitelson et al. (2002)
ARI1 (Anthocyanin Reflectance Index 1)	$ARI1 = (1/R550 - 1/R700)$	Gitelson et al. (2001)
ARI2 (Anthocyanin Reflectance Index 2)	$ARI2 = R800(1/R550 - 1/R700)$	Gitelson et al. (2001)
Other indices		
Red edge 750~700	R750 - R700	Gitelson and Merzylak



		(1997)
Red edge 740~720	$R740 - R720$	Vogelmann et al. (1993)
ZTM (Zarco Tejada and Miller)	$ZTM = (R750 / R710)$	Zarco Tejada et al. (2001)
NDNI (Normalized Difference Nitrogen Index)	$NDNI = \frac{(\log(1/R1510) - \log(1/R1680))}{(\log(1/R1510) + \log(1/R1680))}$	Serrano et al. (2002), Fourty et al. (1996)
NDLI (Normalized Difference Lignin Index)	$NDLI = \frac{(\log(1/R1754) - \log(1/R1680))}{(\log(1/R1754) + \log(1/R1680))}$	Serrano et al. (2002), Fourty et al. (1996), Melillo et al. (1982)
CAI (Cellulose Absorption Index)	$CAI = 0.5(R2000 + R2200) - R2100$	Daughtry (2001), Daughtry et al. (2004)
PSRI (Plant Senescence Reflectance Index)	$PSRI = (R680 - R500) / R750$	Merzlyak et al. (1999)
WBI (Water Band Index)	$WBI = R900 / R970$	Penuelas et al. (1995) and Champagne et al. (2001)
NDII (Normalized Difference Infrared Index)	$NDII = (R819 - R1649) / (R819 + R1649)$	Hardisky et al. (1983) and Jackson et al. (2004)
NDWI (Normalized Difference Water Index)	$NDWI = (R857 - R1241) / (R857 + R1241)$	Gao (1995)
MSI (Moisture Stress Index)	$MSI = R1599 / R819$	Ceccato et al. (2001)
MCARI1	$MCARI1 = 1.2 [2.5 (R800 - R670) - 1.3 (R800 - R550)]$	Haboudane et al. (2004)
MCARI2	$MCARI2 = 1.5 [2.5 (R800 - R670) - 1.3 (R800 - R550)] / [(2 R800 + 1)^2 - (6R800 - 5 (R670)0.5) - 0.5]$	Haboudane et al. (2004)

Previous ground based, airborne and Hyperion sensor based Imaging Spectroscopy Remote Sensing studies revealed its capability in different fields of agricultural research. The science objectives in the field of agriculture are:

- Species/variatal composition (e.g. Basmati vs other rice crop, Bunching crop spreading crop of groundnut) discrimination
- Vegetation or crop type (e.g., pulse crop vs. cereal crop) discrimination

- Crop stage discrimination (vegetative vs reproductive)
- Biophysical properties (e.g., LAI, biomass, yield, density) studies
- Biochemical properties (e.g., Anthocyanins, Carotenoids, Chlorophyll) assessment
- Disease and stress (e.g., insect infestation, drought) assessment
- Nutrients (e.g., Nitrogen) stress assessment
- Moisture (e.g., leaf moisture) stress studies
- Light use efficiency studies
- Net primary productivity studies
- Crop residue studies
- Soil fertility (organic carbon, nitrogen) status assessment
- Soil variability mapping
- Discrimination of horticultural crops

The space imaging spectrometers will be helpful in these fields and hence, can be taken as the research fields. Specific science plan of some of these fields are given below.

#### *Canopy structure studies as basis for crop discrimination*

e.g. an Erectophile (65 degrees) canopy Structure (wheat vs barley)

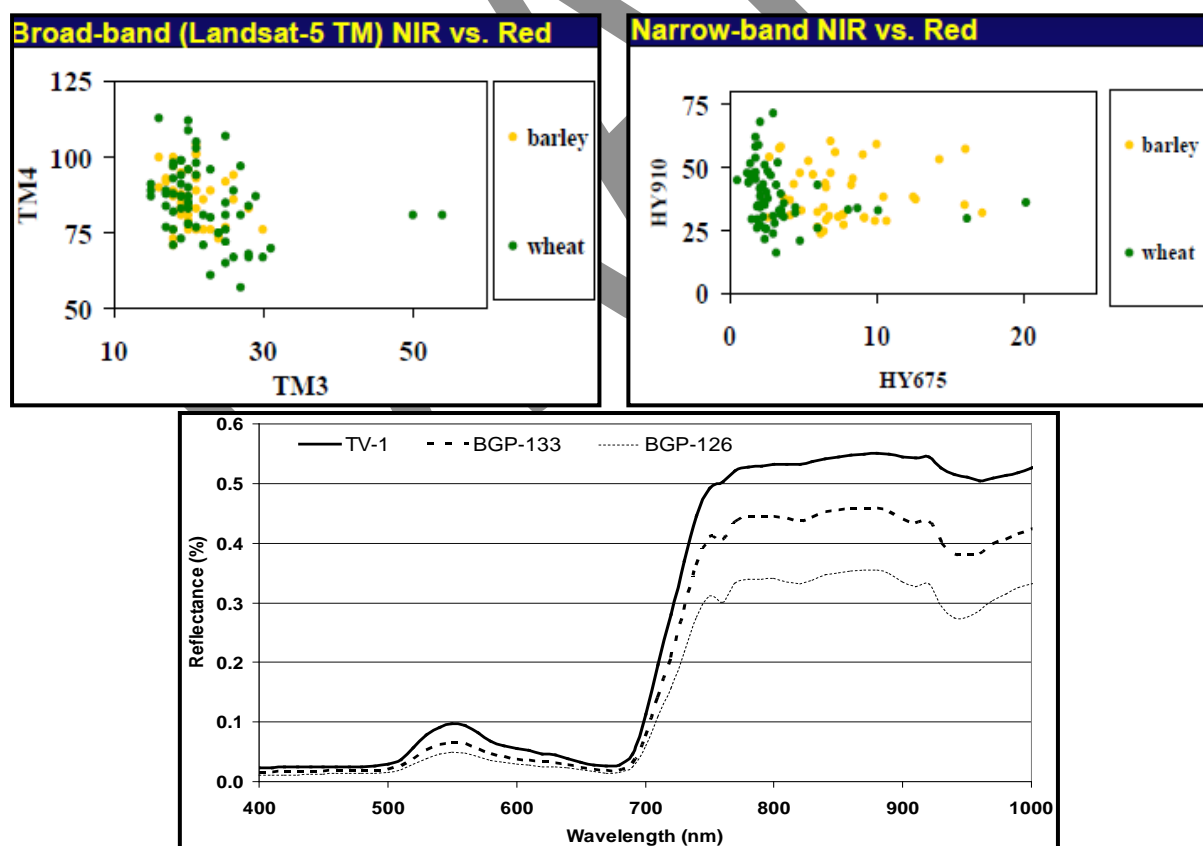


Figure 5 Discriminating vegetation types (above)(Adapted from Thenkabail, 2011) and Tea varieties; TV-1; BGP-133 and BGP-126 varieties of *Camellia sinensis* (lower figure)(Adapted from Amitkumar et al, 2013)

Numerous narrowbands provide unique opportunity to discriminate different crops (Figure 5) and varieties within a crop/species.

### ***Crop stress assessment***

Researchers have often attempted to establish a causal link between measured spectral reflectance and the foliar biochemical composition and/or plant physiology (Shibayama and Akiyama, 1989; Yoder and Pettigrew-Crosby, 1995; Curran et al., 1997, 2001; Blackburn, 1999; Sims and Gamon, 2002; Coops et al., 2003), and their ability to identify crop stress. As the magnitude of change in spectral reflectance in response to stress will vary at different wavelengths, spectral data can be used to unambiguously detect physiological stress in different crop.

### ***Crop stage assessment***

Spectral wavelengths and their importance in the study of vegetation in different growth stages has been reported by several authors. The crop growth results in change in LAI, canopy architecture and components, chlorophyll and other pigment variation and also moisture variation. This results in varying responses at different wavelength, hence the crop stage discrimination is a possibility (Figure 6).

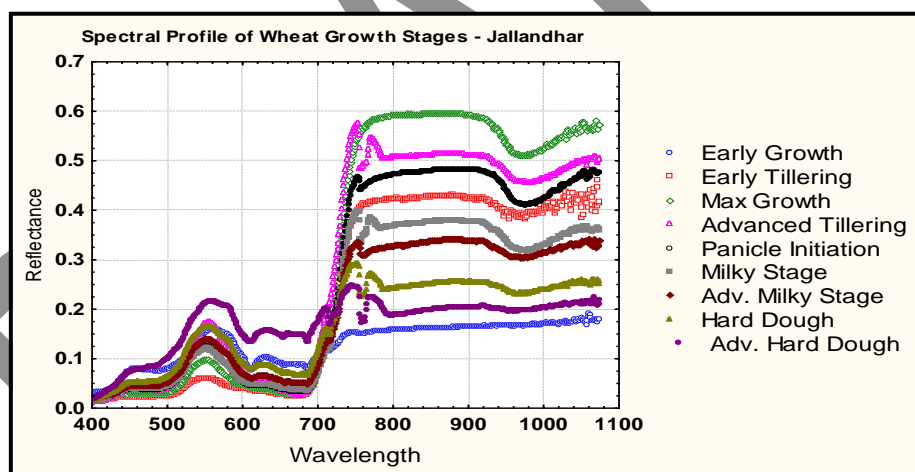


Figure 6 The Spectral curve of various stages of wheat crop obtained using ground based spectroradiometer (Panigrahy and Manjunath, 2011).

### ***Crop nutrient (nitrogen) status***

Nitrogen is one of the most important crop limiting factors and a key parameter for crop monitoring and yield estimation in precision farming (Vigneau et al., 2011). Therefore, the assessment and mapping of total canopy nitrogen (N) content of agricultural crops is very important to optimize nitrogen fertilizer management in agronomy. An efficient and precise use of N-fertilizer is helpful to improve yield, reduce costs and lower environmental pollution at the same time (Ju et al., 2009).

Spectral reflectance of plants in the visible (VIS) and near infrared (NIR) region of the electromagnetic spectrum is primarily affected by plant pigments (e.g. chlorophyll) and cellular structure of the leaves. Plants with limited N-uptake will have a lower chlorophyll concentration which is an indicator for non-optimal photosynthesis (Clevers&Kooistra, 2012). In this context, spectral remote sensing data showed already a high potential for the spatial and non destructive estimation of chlorophyll- and N-concentration. The availability of airborne spectral imaging systems (e.g. HyMap, HySpex, AISA and CASI) in the last years allows acquiring data with high spatial and spectral resolution, supporting the fast assessment of N-status from agricultural fields (Jarmer&Vohland, 2011; Dorigo et al., 2007; Kokaly, 2001).

### ***Crop disease assessment***

In context of insurance claim of agricultural entrepreneurs within disease affected zones, satellite-based disease detection can make an important contribution. The different disease symptoms alter optical, thermal properties of leaves, canopies in different spectral regions through necrotic or chlorotic lesions, premature senescence or browning and canopy dryness (Malthus and Madeira, 1993; West et al., 2003). Hyperspectral observations over a number of bands (>200) at 5–10 nm intervals are quite promising in crop disease detection (Thenkabail et al., 2002; Laudien et al., 2004) as compared to few (4–7) multispectral bands (Kanemasu et al., 1974; Nageswara Rao and Rao, 1982; Franke and Menz, 2007). Spectral discrimination of different diseases was carried out using ground-based, airborne and satellite-based hyperspectral reflectance data for late blight (*Phytophthora infestans*) in tomato (Zhang and Qin, 2004), rice diseases (Qin et al., 2003) and sugarcane orange rust (Apan et al., 2004), respectively. The hyperspectral sensors (e.g. EO-1 Hyperion) have good spatial resolutions (30 m), but have limited swaths (7 km) and low temporal resolution (16–25 days).

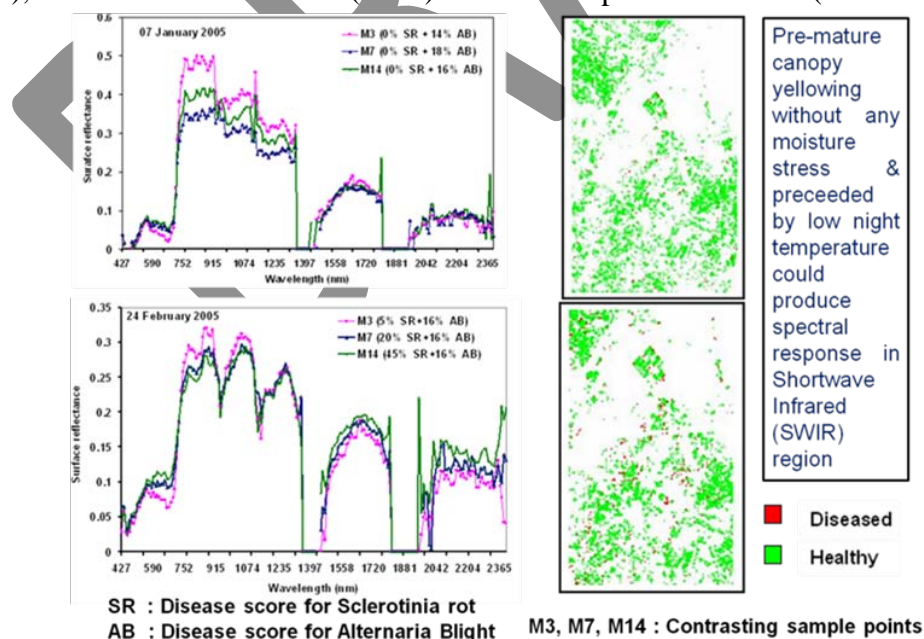


Figure 7. Mustard rot disease detection using EO-1 Hyperion data over Bharatpur, India (Bhattacharya and Chattopdhyay, 2013)

In India, detection of rot disease was carried out by Bhattacharya and Chattopadhyay (2013), Dutta et al (2006) using EO-1 Hyperion data (Figure 7) using two-step discriminant analysis. Among all the hyperspectral indices, a three-band rot index (ROTI) was found to be the better one in field scale rot discrimination (stage-III evaluation). The reduction in fractional canopy cover in diseased patches in 2005 as compared to a normal year (2007) indirectly validated the disease effect

### ***Crop residue studies***

Development of remote sensing indices for assessing crop residue cover has been impeded, because soils and crop residues lack unique spectral signatures in the 400–1100 nm region (Aase and Tanaka, 1991). Crop residues and soils are often spectrally similar and differ only in amplitude at a given wavelength. Shortly after harvest, crop residues are frequently much brighter than the soil, but as the residues weather and decompose they may be either brighter or darker than the soil (Nagler et al., 2000). This makes discrimination between crop residues and soil difficult or nearly impossible using reflectance techniques in the visible and near infrared wavelengths. Research showed that broadband spectral indices are weakly correlated to crop residue cover. Hence the only alternative to discriminating crop residues from soils is based on a broad absorption band near 2100 nm that is associated with cellulose and lignin in crop residues for which spectral data is a necessity. The cellulose absorption index (CAI) based on the ground based spectroradiometer and based on Hyperion data based has shown capability to discriminate crop residue from soil in field studies. This can be extended to large area with the space spectral data in this range.

### ***Parameter retrieval (Bio-physical and bio-chemical)***

The combination of wavebands or SVIs derived from them provide us significantly improved models of vegetation variables such as biomass, LAI, net primary productivity, leaf nitrogen, chlorophyll, carotenoids, and anthocyanins. For example, stepwise linear regression with a dependent plant variable (e.g., LAI, Biomass, nitrogen) and a combination of N independent variables (e.g., chosen by the model from different wave bands) establish a combination of wavebands that best model a plant variable (Figure 8).

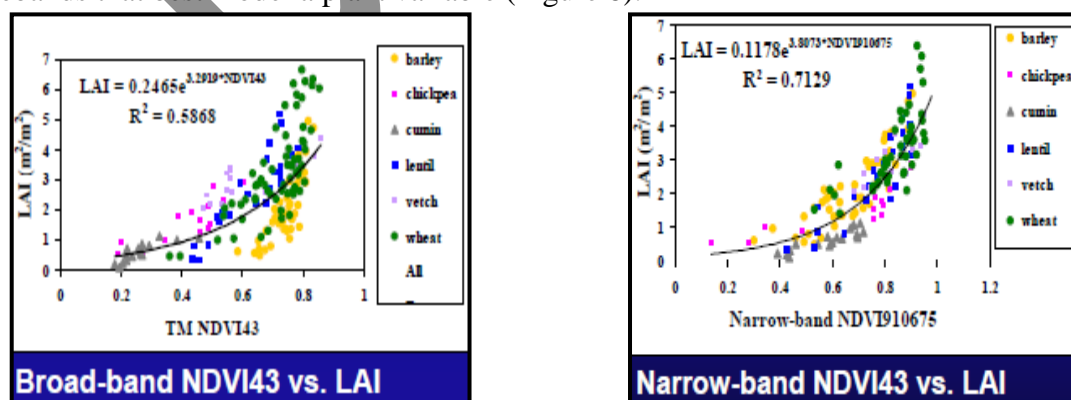


Figure 8 Biophysical parameter relationship with broadband and narrow band NDVI (Thenkabail, 2011).

Red edge is the best index for studying chlorophyll index. For quantitative measurement of plant senescence, difference reflectance of (680-500 nm)/750 nm could be used as this can differentiate the chlorophyll and carotenoids pigments. Figure 9 shows the various spectral signatures of the leaves over its growth phase.

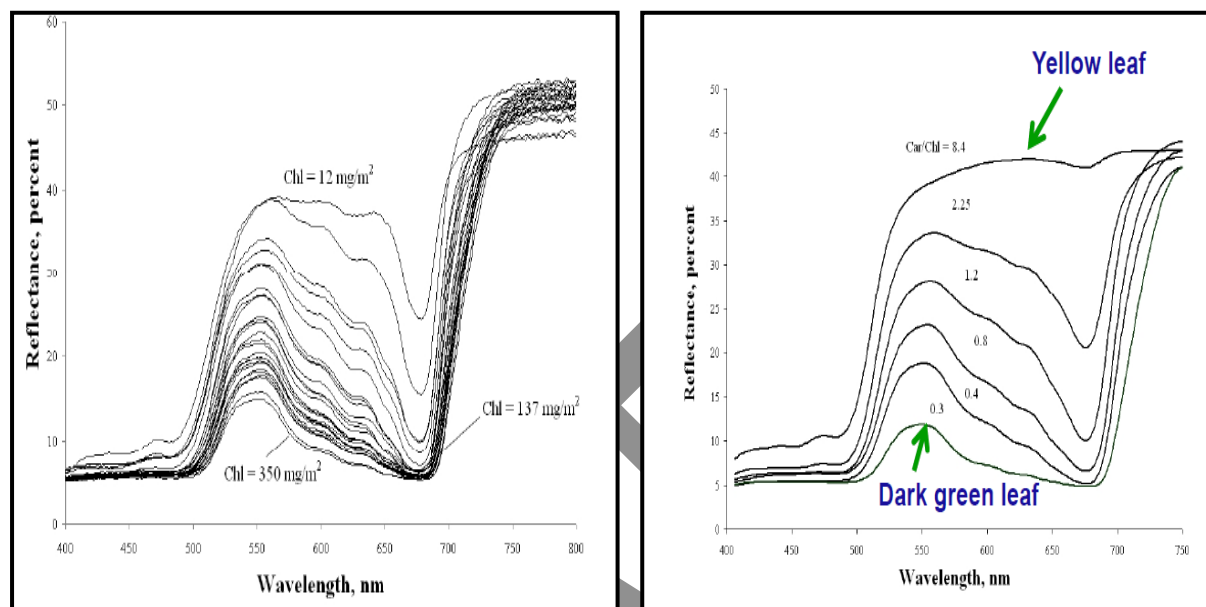


Figure 9 Reflectance spectra of beech leaves at varying chlorophyll concentration and of chestnut leaves –plotted against carotenoids/chlorophyll (chapter 6; Gitelson et al)

### *Soil fertility status and variability mapping*

Typically, all soil spectra show three prominent absorption peaks around 1400, 1900 and 2200 nm. The absorption peaks at 1400 and 1900 nm indicate the first overtone of O–H stretches and the combination of H–O–H bending with O–H stretching and are generally termed as water absorption peaks. The absorption between 2200 and 2300 nm are mainly due to the combination of metal–OH bending and O–H stretching associated with the clay content mineral. Other absorption bands in the NIR region are due to iron oxides between 870 and 1000 nm and carbonates between 2200 and 2500 nm (Clark et al., 1990). Soil Variability Mapping and Fertility Zonation are targeted as main objectives. The importance of various bands is given in Table 2

Table 2 Optimal spectral bands in study of vegetation (Tenkabail, 2011)

Sl. No.		Parameter/Process
A. Blue bands		
1	405	Nitrogen Senescing
2	450	Chlorophyll, carotenoids senescing

3	490	Carotenoids, Light use efficiency (LUE) Stress in vegetation
B. Green bands		
4	515	Pigments (Carotenoid, Chlorophyll, anthocyanins), Nitrogen, Vigour
5	531	Light use efficiency (LUE), Xanophyll cycle, Stress in vegetation, pest and disease
6	550	Anthocyanins, Chlorophyll, LAI, Nitrogen, light use efficiency
7	570	Pigments (Anthocyanins, Chlorophyll), Nitrogen
C. Red bands		
8	650	Pigment, nitrogen
9	687	Biophysical quantities, chlorophyll, solar induced chlorophyll Florescence
D. Red-edge bands		
10	705	Stress in vegetation detected in red-edge, stress, drought
11	720	Stress in vegetation detected in red-edge, stress, drought
12	700-720	Chlorophyll, senescing, stress, drought
E. Near infrared (NIR) bands		
13	760	Biomass, LAI, Solar-induced passive emissions
14	855	Biophysical/biochemical quantities, Heavy metal stress
15	970	Water absorption band
16	1045	Biophysical and biochemical quantities
F. Far near infrared (FNIR) bands		
17	1100	Biophysical quantities
18	1180	Water absorption band
19	1245	Water sensitivity
G. Early short-wave infrared (ESWIR) bands		
20	1450	Water absorption band
21	1548	Lignin, cellulose
22	1620	Lignin, cellulose

23	1650	Heavy metal stress, Moisture sensitivity
24	1690	Lignin cellulose sugar starch protein
25	1760	Water absorption band, senescence, lignin, cellulose
H. Far short-wave infrared (FSWIR) bands		
26	1950	Water absorption band
27	2025	Litter (plant litter), lignin, cellulose p
28	2050	Water absorption band
29	2133	Litter (plant litter), lignin, cellulose
30	2145	Water absorption band
31	2173	Water absorption band
32	2205	Litter, lignin, cellulose, sugar, starch, protein; Heavy metal stress
33	2295	Stress and soil iron content

### Study Sites

The study sites are given in the Table 3

**Table 3: Study sites pertaining to Agricultural and Soil studies**

S.No.	Site	Longitude	Latitude	Remarks	Priority
1	Powarkheda, Madhya Pradesh	77.67	22.78	Soyabean, Rice, Sugarcane	2
		77.78	22.78		
		77.67	22.51		
		77.78	22.51		
2	Nagarjunasagar, Telangana	79.67	17.03	Pest & Disease	1
		79.32	16.91		
		79.70	16.94		
		79.35	16.83		
3	IISC, Muddur, Karnataka	76.56	11.58	Mixed Agriculture	1
		76.66	11.58		
		76.56	11.98		
		76.66	11.98		
4	Surendranagar, Gujarat	71.78	22.56	Cotton stress	1
		71.38	22.55		
		71.78	22.45		
		71.40	22.46		
5	UAS Bangalore	77.55	13.10	Crop Discrimination	1
		77.58	13.08		



		77.58	13.01		
		77.53	13.05		
6	Anand	73.00	22.61	Crop Discrimination	1
		73.06	22.56		
		72.95	22.46		
		72.88	22.53		
7	IARI, Delhi	77.13	28.65	Crop Discrimination	2
		77.16	28.65		
		77.13	28.61		
		77.16	28.61		
8	Hissar, Haryana	75.70	29.31	Crop Discrimination	2
		75.75	29.31		
		75.75	29.26		
		75.70	29.26		
9	ICRISAT, Hyderabad, Telangana	78.23	17.50	Soil	1
		78.26	17.50		
		78.23	17.46		
		78.26	17.46		
10	CRIDA, Hyderabad, Telangana	78.56	17.35	Soil	1
		78.58	17.35		
		78.56	17.31		
		78.58	17.31		
11	ARS, Vuyyuru, Andhra Pradesh	80.81	16.40	Soil	2
		80.83	16.40		
		80.81	16.36		
		80.83	16.36		
12	CSF, Raichur, Karnataka	76.86	15.86	Soil	1
		76.90	15.86		
		76.86	15.81		
		76.90	15.81		
13	Chilika, Odisha	85.54	20.12	Soil	1
		85.45	20.14		
		85.46	19.77		
		85.37	19.79		
14	Bhopal, Madhya Pradesh	77.40	23.67	Soil & Agriculture	2
		77.31	23.67		
		77.39	23.31		
		77.29	23.31		
15	Talala, Junagadh, Gujarat	70.63	21.06	Horticulture orchard	1
		70.65	21.07		
		70.65	21.05		
		70.63	21.06		

### ***Methodology***

The spectral technique of pre-processing (exclusion of bad bands, MNF, atmospheric correction etc.) and classification using SAM etc would be carried out using selected bands.

### ***Expected outcome***

This exercise would lead to development of techniques for spectral measurement usage in newer domains of agriculture especially for India which has large number of crops growing under diverse conditions.

AVIRIS measurements provide access to the full spectral range from 380 to 2510 nm for study of agricultural applications. Figure 10 shows an example data set measure by AVIRIS over agricultural fields in the San Joaquin valley, California. In preparation for the airborne campaign, AVIRIS data sets from North America relevant to agricultural lands of both calibrated radiance and reflectance may be downloaded from the website [http://aviris.jpl.nasa.gov/alt\\_locator/](http://aviris.jpl.nasa.gov/alt_locator/).

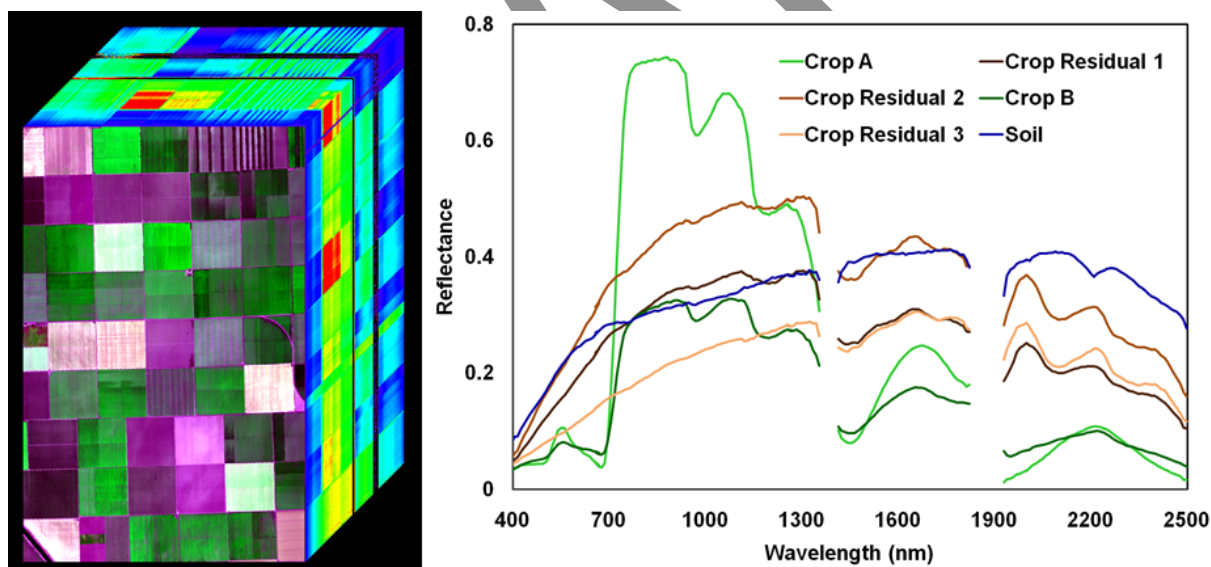


Figure 10. AVIRIS data set measured over an agricultural area and extracted spectra over the range from 380 to 2510 nm (R. Green).

## **WETLANDS ECOSYSTEMS**

The deterioration of the ecological status of continental waters (dams, lakes, lagoons) has become an urgent and growing problem in the last years. Numerous natural and human induced factors contribute to the increase in the concentrations of optically active substances in the water bodies as well as the rise of water turbidity and water temperature. This

processes can lead to algal bloom events, anoxia and even to a dramatic deterioration of water quality. As a consequence, the bio-optical properties and the amounts of the constituents (phytoplankton, detritus, mineral particles and yellow substance) of the water can be modified in short spatial and temporal scales whose investigations are of interest to those responsible for the management of the wetlands especially for reservoirs of drinking water. The investigation and description of the system properties of inland waters, as well as water pollution control and water maintenance, are some of the main tasks in applied limnology. Technological advancements have produced innovative remote sensors, including imaging spectrometers. Spectroscopic imagery is acquired using imaging spectrometers, the simultaneous acquisition of images in many narrow (band width less than 10 nm), contiguous spectral bands as opposed to broad band sensors. As band widths are narrow, local variations in absorption features can be detected that might otherwise be masked within the broader bands of multispectral scanner systems. Imaging spectrometer enable the availability of continuous spectrum than that is available with multispectral instruments. This increases the possibilities of determining the characteristic spectral features for analysis, classification and monitoring cover types and processes.

Various important aspects of wetlands that become amenable to imaging spectroscopy for quantitative estimation, which is otherwise limited to lesser or greater extent with broad-band instruments. The major science objectives are listed below:

- Physical water quality parameters such as transparency, turbidity, suspended sediment concentration.
- Biological characteristics like; chlorophyll concentration.
- Vegetation type/species and density discrimination.
- A new avenue for research to detect the chemical water quality parameters especially that enhance the eutrophication and detect pollutants.

### *Study site*

S.No.	Site	Longitude and Latitude	Remarks
1	Chilika lagoon, Odisha	1) 85.08      19.49 85.03      19.57 85.64      19.91 85.68      19.83 2) 85.03      19.57 84.98      19.65 85.59      19.99 85.63      19.91	Wetland ecosystems

## MANGROVE ECOSYSTEMS

Mangrove forests are found in the intertidal zones of tropical and subtropical coastlines and exist as an ecosystem, comprising estuaries, lagoons, creeks and intertidal mudflats. The ecosystem is sensitive to changes in the local hydrological environment, and the changes are typically manifested through alterations in the species or community composition. Information on the floristic composition of the mangroves using remote sensing data is still at developmental stage. The broadband multispectral remote sensing sensors have been found to be inadequate to discriminate the mangrove classes at genus or species level (Holmgren and Thuresson 1998). In this context, imaging spectroscopy has a significant role to play because of its ability to differentiate subtle differences in biophysical and biochemical attributes of plants. Many studies have been carried out in this direction using airborne and satellite spectral data (Held et al. 2003; Hirano et al. 2003; Lucas et al. 2003; Jusoff 2006; Jensen et al. 2007; Yang et al. 2009; Chakravorty and Chakrabarti 2011; Kamal and Phinn 2011; Kumar et al. 2013). These studies provide mangrove community zonation maps of mangrove forests across the world with better classification accuracies in comparison to broadband multispectral remote sensing data. The potential of in-situ/ field spectral data for discriminating mangrove species using foliar spectral measurements have been explored by various workers (Vaiphasa 2005, 2007; Kamaruzaman and Kasawani 2007; Wang and Sousa 2009; Panigrahy et al. 2012). However, canopy spectra are of greater importance than leaf spectra in the context of airborne/satellite remote sensing. The major science objectives are listed below:

- **Discrimination of mangroves at genus/ species level and mapping of floristic composition of mangrove forests:** this may be highlighted as one of the major benefits of using both airborne and space based imaging spectroscopy. The data may be subjected to different algorithms and statistical tools to identify the most important wavelengths for discrimination between mangrove species. There is also scope for the establishment of spectral libraries for different Indian mangrove species.
- **Discerning wet soils (mudflats) of different inundation levels within mangrove ecosystems** - mudflat is an integral part of a mangrove ecosystem and represents the first physiographic zone in a mangrove ecosystem where phyto-succession begins. This zone exhibits great variability in composition, being flanked by river or creek water on one side and mangrove forest slope on the other. Thus, characterizing the mudflats is also an important requirement in mangrove ecosystem mapping. Algorithms may be developed for obtaining selected wavelengths for differentiating between mudflat classes and creek water and the developed method could be used as an added protocol for discerning wet soils of different inundation levels.
- **Assessment of carbon dynamics/ physiological status of mangrove forests:** a number of vegetation indices are available in the literatures which need to be explored in case of mangrove forests. These are: **(1)for green (live vegetation)** - green NDVI (more sensitive than NDVI to chlorophyll concentration, could be quite useful for

discriminating Rhizophora communities), red edge NDVI, modified red edge simple ratio index, modified red edge NDVI, **(2) for photosynthesis** - total chlorophyll concentration, photochemical reflectance index (measures the down-regulation of photosynthesis during stress such as increase in soil salinity), **(3) for canopy leaf pigments** – carotenoid reflectance indices, normalized difference nitrogen index (relative canopy nitrogen content), **(4) canopy water** – water band index (relative water content, could be quite useful for discriminating sclerophyllous mangrove species having less water content e.g. communities of *Phoenix paludosa* from species with considerable amount of achlorophyllous water storage tissues e.g. *Sonneratia* communities), moisture stress index, normalized difference water index, normalized difference infrared index, spectroscopic water absorption metric, **(5) non-photosynthetic vegetation** – cellulose absorption index (relative amount of dry plant material), normalized difference lignin index (relative canopy lignin content), plant senescence reflectance index [plant litter (dry and decomposing leaves)].

- **Mangrove forest health:** the health of mangroves may be reduced by stress agents that can be biological (e.g., disease, attack/predation) or physico-chemical (e.g., increase in soil salinity due to reduction in fresh water influx) in origin. Typical responses to stress include structural deformity (stunted growth), changes in internal biochemistry (e.g. changes in leaf pigment concentrations and canopy water), and partial or complete degradation of plant material (e.g., reductions in crown leaf area). By exploiting known sensitivities in specific wavelength regions to biochemical parameters, changes in mangrove forest health may be detected using imaging spectroscopy measurement. A number of vegetation indices can be used in the assessment of mangrove forest health/ condition. Some of these are - red edge vegetation stress index (identifies inter- and intra-community multi-temporal stress trends based on spectral changes in upper red-edge geometry), wavelength position of red edge [main inflection point of the slope between red and NIR. A shift towards shorter (longer) wavelengths indicates increasing stress], red edge position index (sensitive to changes in chlorophyll concentration).
- Monitoring of mangrove forests for deforestation or regeneration – significant areas of mangrove forests have been destroyed across the world for various uses (e.g., aquaculture), but also because of natural events, including cyclones and tsunamis. Mangroves are also responding to fluctuating sea levels as a consequence of climatic change. At a regional level and for mapping and monitoring changes in mangrove forest extent associated with deforestation or regeneration, multispectral remote sensing data acquired by space sensors are generally adequate. However, in many areas, mangrove extent might remain similar, but changes in species composition, structure, and biomass can occur, with these reflecting diversification, encroachment or loss of species, and growth and dieback of individuals. Therefore, more detailed baseline datasets of species distributions as well as structure and biomass are required in addition to extent, with the level of details required depending upon the nature and

extent of change. For this purpose high spatial resolution imaging spectroscopy data might prove to be quite useful.

### **Study area**

The study sites are given in the Table 5.

Table 5: Survey Area for mangrove ecosystem study

S.No.	Site	Longitude and Latitude		Priority
1	Sunderban, West Bengal (Mangroves)	88.57	21.75	1
		88.71	22.18	
		88.80	22.12	
		88.68	21.72	
2	Bhitarkanika, Odisha (Mangroves)	86.91	20.83	1
		86.99	20.79	
		86.76	20.68	
		86.84	20.63	
3	Pichavaram, Tamil Nadu (Mangroves)	79.71	11.51	1
		79.77	11.52	
		79.77	11.39	
		79.83	11.39	
4	Sunderban, West Bengal (Mangroves)	1)		1
		88.27	21.88	
		88.85	21.88	
		88.86	21.78	
		88.27	21.78	
		2)		
		88.57	21.75	
		88.71	22.18	
		88.80	22.12	
		88.68	21.72	

AVIRIS measurements have been used in North America to study the coastal zone of the Gulf of Mexico as shown in Figure 11. In preparation for the airborne campaign, AVIRIS data sets from North America relevant to wetland ecosystems of both calibrated radiance and reflectance may be downloaded from the website [http://aviris.jpl.nasa.gov/alt\\_locator/](http://aviris.jpl.nasa.gov/alt_locator/).

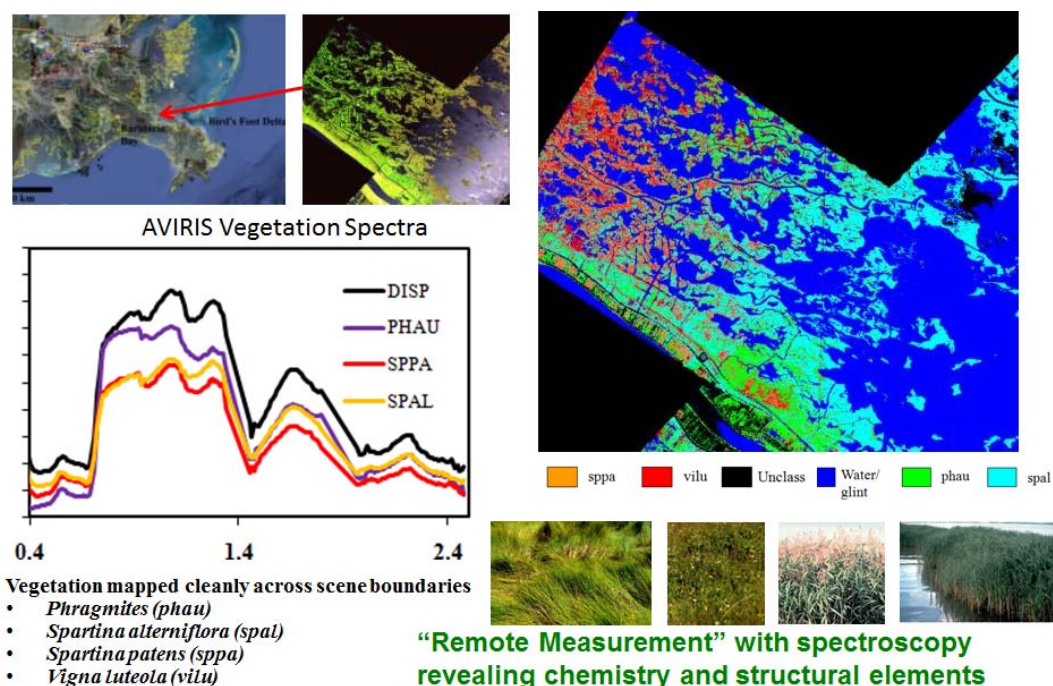


Figure 11. Example AVIRIS measurement along the Gulf of Mexico for species mapping and study of wetland ecosystems (D. Roberts, UCSB).

## 4.2 FOREST ECOSYSTEM

Forest covers more than one fifth of geographical area of the country. It constitutes a large part of natural resources. Additionally forest serves as major regulator of earth's environment. Remote sensing based forestry applications related to optical remote sensing are in matured state. Major concern was to assess the forest type and density on national level using IRS series of data. In recent years, advances have been made in classifying vegetation using optimal spatial resolutions (Marceau et al. 1994) red-edge, first derivatives and green peak statistical indices (Portigal et al. 1997). But lacking firsthand experience, it will be interesting to see the applicability of such techniques in a complex scene such as that presented by a tropical forest canopy.

Despite the creation of spectral libraries for various plant species, the unique identification of many species in natural ecosystems has proven difficult due to the numerous problems present in real-world measurements, such as angle of view, atmospheric properties, spectral mixture, moisture content, illumination angle, plant assemblage to mention just a few. Variability can occur within a species due to microclimates, soil characteristics, precipitation, topography and a host of other environmental factors (Portigal et al. 1997), therefore one species pure spectral library may not hold good. Several species may actually have quantitatively similar spectra due to the spectral signature variation present within a species (Price, 1994). In addition, stress factors such as air pollution, heavy metals and drought can change the spectral properties of foliage (Westman and Price 1987). In short, spectral signatures may not be unique. The spectral separability of vegetation provides special difficulties because its spectral behavior is described by a small number of independent variables (Price, 1992). Furthermore, both foliage age (Gausman 1985, Roberts et al. 1998)

and position in the canopy (Danson 1995) have been shown to cause substantial differences in the spectral signatures of some species. Colonization by leaf pathogens (epiphylls) and climbers may also change the spectral response, especially among older leaves (Roberts et al. 1998). Some of these issues can be solved through modeling and contextual information and imaging spectroscopy can potentially be used for discrimination at species level and community level using the potential of narrow band data.

The response of vegetation reflectance spectra in visible wavelengths (400 – 700 nm) is primarily determined by the composition and concentration of chlorophyll a, chlorophyll b and the carotenoids (Tucker and Garrett 1977). Furthermore, the response of reflectance spectra in the near-infrared wavelengths (700–1300 nm) is a function of the number and configuration of the air spaces that form the internal leaf structure (Danson 1995). In summary, the reflectance of vegetation from different species is highly correlated due to their common chemical composition (Portigal et al. 1997). It will be interesting to combine and use the response of other biochemical properties from 1300 – 2510 nm and complex indices can be attempted for species level classification of forests. With the availability of narrow bands within 380-2510 nm wavelength from airborne/space platforms, research in this area will become more intensive and new techniques and indices of assessment of the data will be explored. A primary advantage of imaging spectroscopy is its ability to provide measurements of forest chemistry. Major elements of chemistry area: chlorophyll a, b, leaf water, cellulose, pigments, lignin canopy chemistry can be used to estimate new and old foliage, detect damage, identify trees under stress or diseased, and map chemical distributions in the forest. This property will enable the forest researchers in applications related to forest health, stress, detection of diseases, and assessment of nitrogen and heavy elements. The concentration of nitrogen in foliage is strongly related to rates of net photosynthesis, and hence carbon uptake across a large number of species. This represents a strong meaningful link between terrestrial cycle of nitrogen and carbon (Field et al, 1986, Reich et al, 1999, Wessman et al, 1988). These variables or vegetation indices will be useful for coming out with plant functional types, which is still nascent area of research through remote sensing. More insights to ecosystem function, such as biochemical fluxes and processing will require advanced vegetation indices. These indices may give elucidation of bio-chemical fluxes in terrestrial ecosystem functions relevant to the nitrogen and carbon cycle components.

Biomass burning is another area where imaging spectroscopy will be of immense use. Imaging spectroscopy measurement would be able to provide sub pixel burnt scar. To model the fire risk potential, the dry or senescent carbon indices designed to provide an estimate of the amount of carbon in dry states of lignin and cellulose can be used to know the state of forests. Lignin is a carbon-based molecule used by plants for structural components; cellulose is primarily used in the construction of cell walls in plant tissues. Dry carbon molecules are present in large amounts in woody materials and senescent, dead, or dormant vegetation. These materials are highly flammable when dry. Increases in these materials can indicate when vegetation is undergoing senescence. Vegetation indices can be used and developed for fire fuel analysis and detection of surface litter based on the pure spectra of lignin, cellulose and water content. The Cellulose Absorption Index is one such vegetation index which



indicates exposed surfaces containing dried plant material. Absorptions in the 2000 nm to 2200 nm range are sensitive to cellulose. Applications also include crop residue monitoring, plant canopy senescence, fire fuel conditions in ecosystems, and grassland grazing management. The Moisture Stress Index (MSI) is a reflectance measurement that is sensitive to increasing leaf water content. As the water content of leaves in vegetation canopies increases, the strength of the absorption around 1599 nm increases. Absorption at 819 nm is nearly unaffected by changing water content, so it is used as the reference. The MSI is inverted relative to the other water VIs; higher values indicate greater water stress and less water content. Moreover, this can also help in monitoring phenology of gregarious flowering species that can also lead to understanding of the biochemical processes of plants and can provide significant clues about the sensitivity of such phenomenon with various factors that alters the flowering mechanisms. There are several habitats in India which are known for mass flowering of species and holds key species that have economic importance. Applications include canopy stress analysis, productivity prediction and modeling, fire hazard condition analysis, and studies of ecosystem physiology. Following are the objectives under this theme:

- Species / Community level mapping of forests
- Identification of physiologically quantitative vegetation stresses
- Development of fuel moisture index for fire risk modeling
- Quantification of foliar biochemistry and fluxes
- Understanding flowering phenology, and
- Development of Plant Functional Types

### **Study area**

The study sites are given in the Table 6

S.No.	Site	Longitude and Latitude		Remarks	Priority
1	Kanha National Park, Madhya Pradesh	80.53	22.39	Forest Ecosystems	2
		80.62	22.43		
		80.80	22.20		
		80.72	22.16		
2	Kass Plateau, Maharashtra	73.69	17.82	Forest Ecosystems	2
		73.77	17.87		
		73.88	17.58		
		73.96	17.62		
3	Sholayar R F, Kerala	76.58	10.51	Forestry	1
		76.67	10.53		
		76.60	10.16		
		76.68	10.16		
4	Shoolpaneshwar R F, Gujarat	73.65	21.88	Forestry	1
		73.75	21.86		
		73.66	21.51		
		73.75	21.51		
5	Himachal Pradesh	76.23	31.27	Forestry	

		76.32	31.30		1
		76.47	30.95		
		76.55	31.02		
6	Yallapur, Karnataka	74.56	14.75		1
		74.90	14.75		
		74.56	15.21		
		74.90	15.21	Forestry	
7	Vansda, Gujarat	73.48	20.82		1
		73.44	20.82		
		73.48	20.73		
		73.44	20.73	Forestry (Phenology in forest)	
8	Himachal Pradesh	76.48	31.03		1
		76.46	31.08		
		76.48	30.99		
		76.46	30.99	Forestry (Tropical forest Classification)	
9	Madumalai, Tamil Nadu	76.46	11.73		1
		76.55	11.73		
		76.46	11.38		
		76.56	11.38	Phenology and forest stress	

### *Expected outcome*

With the advent of sensors capable of collecting high-spectral-resolution radiance data between 380-2510 nm with about 10 nm spectral resolution and at 30 m spatial resolution the expectation is that, if measurements are made with sufficient signal to noise ratio to avoid spectral mixing, most types of vegetations could be remotely identifiable. Detail mapping of species level, can help us identify spread of invasive species in an area as well as modeling the presence of similar spectra elsewhere for identifying unknown locations of same. Developing stress indices and full understanding of foliar biochemistry will provide clues for ecosystem modeling in terms of nutrient recycling as well as for fire risk modeling. This technology can thus help in characterizing vegetation to a further level not only for scientific understanding but also for ecosystem modeling and conservation related issues.

AVIRIS imaging spectrometer measurements have been used for more than a decade to measure the properties of forest ecosystems. Figure 12 shows an example of species mapping for a forested ecosystem in North America. In preparation for the airborne campaign, AVIRIS data sets from North America relevant to forest ecosystem of both calibrated radiance and reflectance may be downloaded from the website [http://aviris.jpl.nasa.gov/alt\\_locator/](http://aviris.jpl.nasa.gov/alt_locator/).

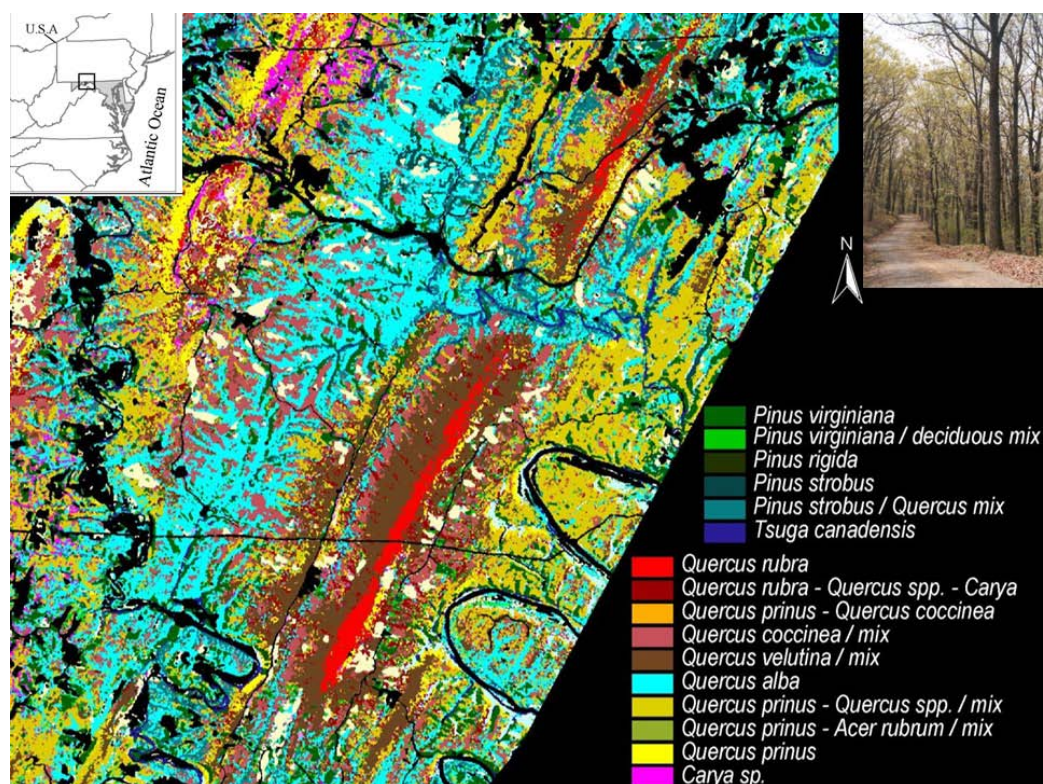


FIGURE 12. DETAILED SPECIES MAPPING IN A FORESTED ECOSYSTEM WITH AVIRIS MEASUREMENTS (P. TOWNSEND).

### 4.3 CORAL REEF ECOSYSTEMS

Imaging spectroscopy of coral reef ecosystems present an opportunity to understand spectral properties of the constituent components through per-pixel optical analysis. When viewed from space, the back-scattered signal from coral reef at the sensor, includes signals from three major components: i) the air-water interface, ii) the water column and iii) the bottom substrate which altogether define the vertical structure of the coral reef (Hedley, 2013). This vertical structure varies over space and time due to atmospheric conditions, water column depth and properties and diversity of bottom substrate. Bottom substrates in case of coral reefs include both biotic and abiotic components commonly termed as benthic and litho-substrates. Benthic substrates include three major groups of benthic biota: i) coral; ii) macroalgae and iii) seagrass while the litho-substrates characterize the sedimentary deposits in a coral reef like coralline sand, sand, silt, mud, coral rubbles, coral boulders, etc. based on their grain sizes. High bottom substrate diversity at sub-meter scale, under variable water depths and water quality makes coral reef ecosystems a complex target for analytical optical algorithms.

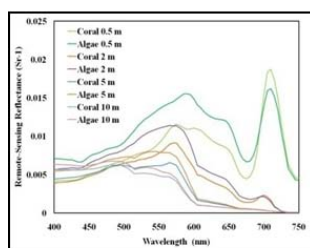
Imaging spectroscopy of coral reefs helps in benthic patch /diversity mapping as compared to conventional habitat mapping in terms of eco-geomorphological zones based on high (spatial) resolution, multi-spectral data. The spectral imaging of coral reef environments shall have the following objectives:

- **Mapping of Submerged Macrophytes/Macroalgae in a coral reef environment:**In coral reef environment three major groups of macroalgae: Chlorophyta, Phaeophyta and Rhodophyta compete for space with corals and possess definite spectral properties due to their inherent pigments: chlorophyll, peridinin, fucoxanthin, phycoerythrin, phycocyanin, etc. Macroalgal groups have homogeneous spatial spreads as compared to coral occupancy and can thus become a suitable substrate to study through space based spectral imaging.
- **Habitat discrimination into benthic and litho-substrate zones:** Availability of a full-range instrument will help in identification of benthic and litho-substrate dominated zones at per pixel level. However, success rate in identifying the dominant substrate per pixel may prove difficult at times as the spatial resolution (30 m) is becoming coarse. This will need a robust spectral unmixing technique and concurrent/synchronous field observations.
- **Water column characterization and depth estimation:** Radiative Transfer (RT) modeling based algorithms can help to characterize the water column properties and estimate the vertical depth of water over a homogeneous bottom substrate.

***Study site:***

Pirotan reef, Gulf of Kachch (UL: 22 38 N, 69 55 E; UR: 22 38 N; 69 60 E; LR: 22 35 N; 69 60 E; LL: 22 35 N; 69 55 E). Since the timing of aerial survey of this site needs to be synchronized with the low tide exposure of the coral reef during daylight, the possible windows (months) planned for the aerial flight shall depend upon the dates and timings. October/November, 2014 onwards the same can be planned on this site to avoid cloud cover and monsoon effects.

AVIRIS measurement in the states of Hawaii and in Florida have been used to investigate the status of coral reef and the benthic habitats of the coastal zone. Figure 13 shows an example AVIRIS data set and analysis from Kaneohe Bay, Hawaii. In preparation for the airborne campaign, AVIRIS data sets from Hawaii relevant to coral reef ecosystems of calibrated radiance may be downloaded from the website [http://aviris.jpl.nasa.gov/alt\\_locator/](http://aviris.jpl.nasa.gov/alt_locator/).



- Composition
- Condition
- Productivity
- Bathymetry
- Water quality



AVIRIS Image of Kaneohe Bay, HI

Classification of the bottom of coastal zones and coral reef types

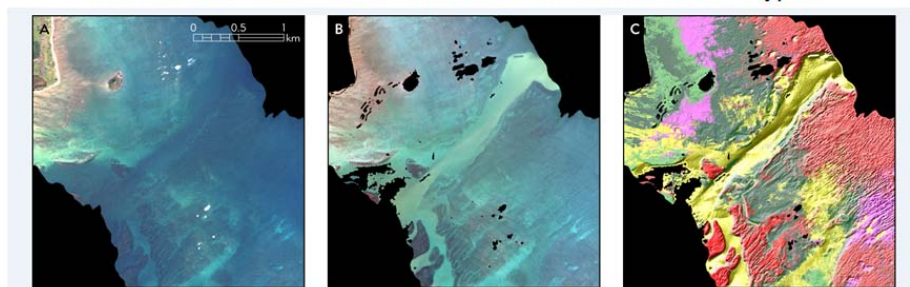


Figure 13. Example AVIRIS data set and analysis for coral reef characterization and benthic habitat measurement. (Eric Hochberg)

#### 4.4 MINERAL EXPLORATION

**Goal: Identification of mineral prognostic zones for base metals & bauxite deposits using imaging spectroscopy measurements**

India is rich in its mineral resources and mining is an important industry next only to agriculture and is critical to the national development involving both big and small mining industries. The mineral resources of India include four fuel minerals (e.g., coal, petroleum, natural gas and atomic minerals), eleven metallic minerals (e.g., iron, aluminium, lead, zinc, chromite, gold, silver etc.), fifty two non-metallic minerals (e.g., bauxite, gypsum, limestone, dolomite etc.) and twenty two minor minerals. It is third in the production of coal, lignite, and chromite, fourth in iron ore, sixth in bauxite and manganese ore. India produces almost one fourth of the total mineral resources of the world. It is largest in the production of mica in the world. Further exploration is required using integration of conventional and modern techniques. New mineral deposits needs to be explored to meet ever-increasing demand of the industries.

The key elements in planning a mineral exploration program prior to undertaking intensive field exploration activities are: Obtain preliminary details of a geographic area through lithological mapping. Identifying the potential targets with particular mineral. Lithology and structural history of study areas. Mineralisation is always confined to specific geological environment. Various guides for mineral exploration are used. Geologists have been exploring for minerals using conventional techniques of exploration such as geological mapping followed by geophysical and geochemical investigations, pitting, trenching,

exploratory drilling, estimating reserves etc. Satellite data are usually utilised to update the existing geological/structural maps at large scale. Minerals that can be successfully identified with spectral images are: OH-bearing minerals, carbonates, sulfates, olivines, pyroxenes, iron oxides and hydroxides (Table 7 & Table 8).

Table 7 Spectral signatures of minerals having diagnostic spectral properties

Mineral/Mineral Group Name	Signature details and cause of the signature
Limonite (Iron Oxide)	Absorption due to Fe-O charge transfer effect (0.7 $\mu\text{m}$ for ferric ion).
Quartz	Absorption in Thermal –TR region (Si-O vibration absorption of tectosilicate in 10 $\mu\text{m}$ ).
Pyroxenes and Olivines	Absorption in 0.7, 1,2 $\mu\text{m}$ for absorption caused in ferrous and ferric ion for crystal field and charge transfer effect. Chain silicate has Si-) absorption in 11.5 $\mu\text{m}$ .
Amphiboles	Absorption signature due to Iron occur in the VNIR (0.4, 0.5 $\mu\text{m}$ region and also in SWIR region (1,2 $\mu\text{m}$ ). absorption mainly due charge transfer effect.
Micas and Clay	Absorption due to vibrational absorption of Hydroxyl ion in the SWIR region (1.4, 1.9 $\mu\text{m}$ ) and those due to vibration in AL-OH, Mg-OH molecules in clay in SWIR region (2.1-2.4 $\mu\text{m}$ ).
All Carbonates	1.9-2.35 $\mu\text{m}$ , latter being more intense for combination overtone of Vibration of Co <sub>3</sub> molecule.

Table 8 Spectral signature of few major rocks

Broad Rock Type	Category	Signature details and cause of signature
IGNEOUS	Granite	A) Absorption bands in 1.4, 1.9, 2.2 $\mu\text{m}$ B) Absorption in 0.7 and 1 $\mu\text{m}$ corresponding to absorption for crystal field effect/charge transfer
	Mafic rocks	B) 0.7 $\mu\text{m}$ and 1.0 $\mu\text{m}$ for absorption bands for ferrous Fe+2 and Fe+3 ion occurs mineral like pyroxene, amphibole, Olive.
	Ultra mafic rocks	A) Absorption band at 1.0 $\mu\text{m}$ and 2 $\mu\text{m}$ specially for Fe+2 as observed in rock like Dunite.
SEDIMENTARY	Sandstone	A)Absorption for Ferrous and Ferric ions. Fe rich sandstone produce absorption in 0.87. Greywacke produce absorption due to fundamental /overtone vibration of clay minerals in 2.1-2.4 $\mu\text{m}$ .
	Shale	A)Mostly due to vibrational overtone combination in OH and H <sub>2</sub> O and also due to



		vibrational absorption for AL-OH and Mg-OH in 2.1 $\mu\text{m}$ and 2.4 $\mu\text{m}$ respectively.
	Limestone and Dolomite	A) Absorption in 1.9-2.35 $\mu\text{m}$ , latter being more increase for combination overtone to the substitution of $\text{Mg}^{2+}$ by $\text{Fe}^{2+}$ .
METAMORPHIC	Schist	A) Absorption signature in 0.7, 1, 2 $\mu\text{m}$ general due to ferrous and ferric ion and 2.1, 2.3, 2.4 for vibrational absorption for AL-OH, MG-OH bond in clay mineral.
	Marble	A) 1.9-2.35 $\mu\text{m}$ , latter being more intense for combination overtone of vibration $\text{CO}_3$ molecule.

The identification of these minerals provides a framework for exploration of precious and base metals, diamonds, etc. Satellite images indicate some of the guides like zones of crustal weakness such as faults, fractures, folds, lithocontacts, shear zones and circular features. These form favorable passages for mineralizing solutions. The tonal and vegetation anomalies on satellite images usually indicate alteration zones. Identification of hydrothermal alteration zones is also a useful guide as alteration halo is much more widespread of rocks surrounding a mineral deposit that are caused by solutions that formed the deposit. Recent trends are towards making use of spectral data in discrimination of surface exposures of minerals using digital classification techniques and identifying surface mineral assemblages as a clue leading to identification of mineral prognostic zones. Mineral exploration using combination of EO data sets, field observations and integration of remote sensing derived information, updated geological and structural information along with geochemical, geophysical, test pitting and test drillings in GIS environment is envisaged to be an improved technique. The major objective of this study is to demonstrate application of spectral data in lithological discrimination and mapping for mineral exploration in selected metallogenic provinces. Detailed objectives are as follows:

- To evaluate the potentials of spectral data in discriminating surface minerals/rock types having diagnostic spectral features.
- To understand effect of weathering and soil on the spectral behavior of different rock types.
- Upgradation of existing geological map using imaging spectroscopy measurements.
- Utilization of spectral and other remote sensing data for identifying guides for mineral exploration, such as, lithological, structural, geomorphological,

stratigraphical, geobotanical etc. and correlation of these guides for identification of mineral prognostic zones.

### Study Area

Following study areas are identified on the basis of known mineral occurrences, exposed outcrops, varied lithological/geological set-ups (in order of preference) and to explore for intervening and extension zones of known occurrences:

Table 9 Survey area for geological applications

S.No.	Site	Longitude and Latitude		Remarks	Priority
1	Jahazpur I, Rajasthan	74.94 75.31 75.37 75.00	25.41 25.72 25.65 25.33	Geology (Lead-Zinc- Copper belt)	1
2	Jahazpur II, Rajasthan	75.37 75.43 75.06 75.00	25.65 25.58 25.26 25.33	Geology (Lead-Zinc- Copper belt)	1
3	Zawar Mines, Rajasthan	73.65 73.77 73.60 73.70	24.37 24.36 23.91 23.90	Geology (Silver, Cadmium, lead- zinc)	1
4	Ambaji, Gujarat	72.61 72.97 72.69 73.06	24.15 24.50 24.08 24.44	Geology (Poly metallic base metal)	1
5	Pur Banera, Rajasthan	74.32 74.64 74.73 74.40	25.17 25.52 25.46 25.11	Geology (Lead-Zinc)	1
6	Udaipur, Rajasthan	73.84 73.75 73.72 73.61	24.58 24.59 24.24 24.25	Geology (Silver, Cadmium, lead- zinc)	1
7	Bhukia, Rajasthan	73.86 74.56 73.86 74.56	23.60 23.60 24.43 24.43	Geology (Gold)	2
8	Sakoli, Maharashtra	79.25 80.25 79.25 80.25	20.50 20.50 21.50 21.50	Geology (Tungsten)	1
9	Hutti-Muski Area, Karnataka	76.5 76.88 76.5 76.88	15.66 15.66 16.33 16.33	Hydrothermal alteration  Gold	1



		76.82	16.36		
		76.74	16.4		
		76.66	16.04		
		76.58	16.07		
10	Wajrakarur, AP	77.38	15.03	Geology (Diamonds)	1
		77.40	15.03		
		77.38	15.75		
		77.40	15.75		
11	Sitampundi, Tamil Nadu	77.99	11.27	Geology (Igneous complex)	
		77.99	11.21		
		77.87	11.209		
		77.87	11.269		
12	Jhadia, Gujarat	73.22	21.77	Mineralogy	
		73.298	21.71		
		73.03	21.45		
		72.95	21.51		

### ***Data Sources***

The imaging spectrometer data sources are Hyperion (EQ-1) and AVIRIS from USA or HyMap from Australia. The data available freely at the moment is limited. Imaging spectrometer data needs to be collected by airborne campaigns for specific areas of interest and locations where there is no vegetation cover and rocks in general are exposed. Accordingly few sites have been selected for detailed investigations as described above.

### ***Methodology***

The major steps envisaged are as follows:

- Collection of ground data using spectroradiometer for identifying spectral signatures of rocks/minerals.
- Study of Satellite-derived spectral reflectance data for identification of spectral signatures of rocks and minerals.
- Application of advanced spectral analysis techniques such as MNF (Minimum Noise Fraction Transform), Pixel Purity Index estimation, End member spectra collection etc.
- Identifying best possible band combination for detection of absorption minima of a particular rock/mineral.
- Matching of image derived end member spectra with available spectral libraries such as USGS, JPL, JHU etc.
- Supervised classification using Spectral Angle Mapper (SAM), Spectral Feature Fitting (SFF), Mixture Tuned Matched Filtering (MTMF) and Spectral Unmixing Techniques.
- Synergetic use of various sensors data shall be made for identifying guides for mineral exploration. Correlation with known mineralized zones shall be studied for

lithological, structural, stratigraphic guides and mineral prognostic zones for unknown regions shall be identified.

- Validation shall be carried out for identified mineral prognostic zones.

### ***Outcome/Results expected***

- Methodology for analyzing imaging spectroscopy data for geological/mineral studies.
- Understanding spectral characteristics of mineral assemblages in identified study areas.
- Spectral library for minerals occurring in specific sites studied.
- A classified mineral map of each of the study area
- Integrated modeling using geoinformatics and identification of mineral prognostic zones.
- Validation using conventional geological/geochemical/geophysical investigations

The spectral signatures of minerals have been measured by AVIRIS for more than two decades. Figure 14 shows an example of the spectral signature diversity for a number of mineral found on the Earth's surface. Figure 14 show mineral maps for the Cuprite region of Nevada using the Tetracorder algorithm. In preparation for the airborne campaign, AVIRIS data sets from North America relevant to geology and mineral mapping may be downloaded from the website [http://aviris.jpl.nasa.gov/alt\\_locator/](http://aviris.jpl.nasa.gov/alt_locator/) as calibrated radiance and atmospherically corrected reflectance.

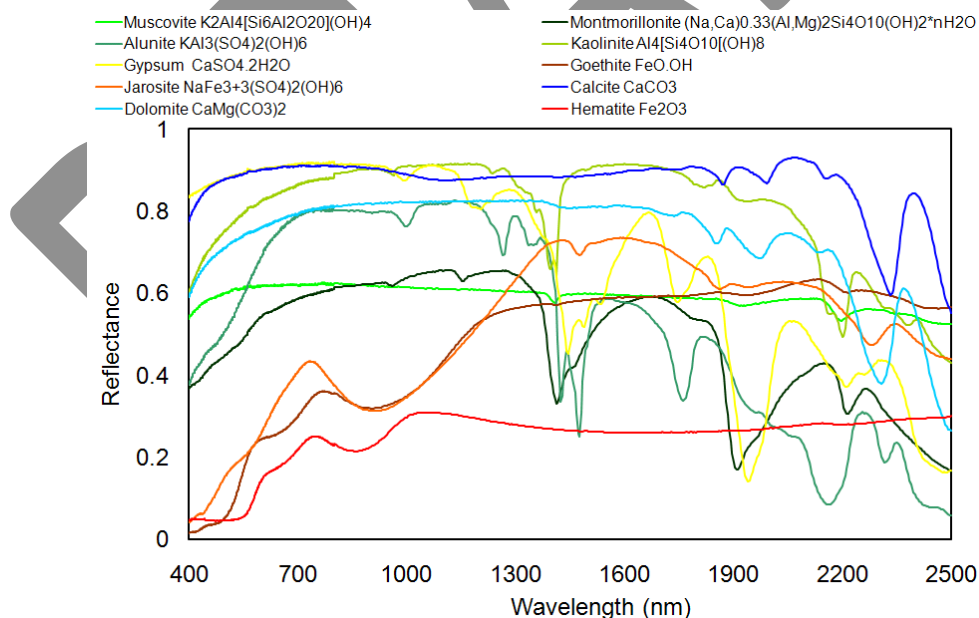


**Figure 14. Spectra of minerals found at the Earth's surface over the AVIRIS spectral range that reveal the diversity of spectral information for mapping surface mineralogy with imaging spectroscopy.**

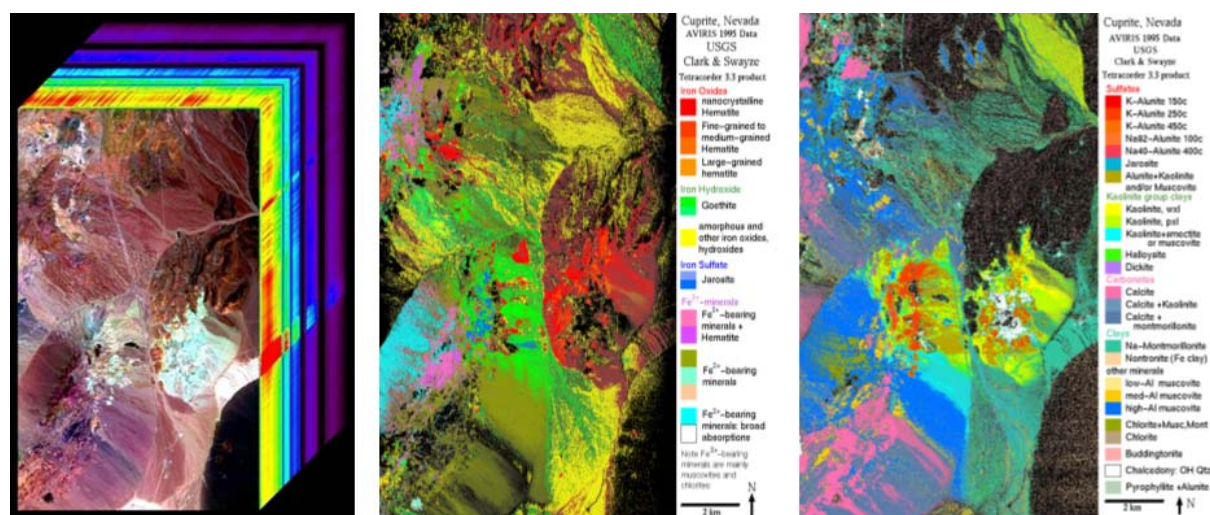


Figure 14. Example surface mineral maps generated from AVIRIS measurements using the Tetracorder algorithm in the region near Cuprite, Nevada (Roger Clark, USGS).

#### 4.5 SNOW AND GLACIER

Imaging spectrometer data collected using airborne or ground observations are useful for characterisation, quantification, identification and detection of subtle changes in snow reflectance due to the influence of snow grain size, contamination, moisture, snow depth, slope aspect, and snow mixed objects. The overall purpose is to identify sensitive/suitable wavelengths for automated mapping of snow types and estimation of snow pack characteristics and understand influence on albedo using imaging spectrometers mounted on space platforms.

Albedo estimates will help in estimating energy balance over snow and estimation of radiation budget over the Himalayan region. Albedo from snow cover in winter effects radiation budget which governs the Indian south-west monsoon and snow melt. Snow melt gets mixed up with rainfall runoff during S-W monsoon season and N-E monsoon seasons. Precise estimates of onset and amount of snow melt at different topographic locations is a gap in Himalayan cryospheric studies.

Snow grain size is the primary parameter snow pack characteristic controlling the albedo. It is crucial to calculate absorption of solar radiation due to snow pack characteristics and quantify albedo. The optical properties depend upon individual constituents in snow, the location and frequency of scattering and absorption events, and radiation's angle of incidence. Anything that changes the probability of an incident photon being scattered or absorbed within snow and ice will have an effect on the spectral albedo. For instance, if a strongly absorbent impurity is added to snow/ice (e.g. soot) it will increase the probability of an incident photon being absorbed and will reduce the snow/ice albedo. Everything else being equal, if the numbers of air bubbles in a sample of glacier ice are increased, the probability of an incident photon scattering out of the ice will increase and so will its albedo.

Rate of snow grain growth is exponentially proportional to the snow temperature and therefore, changes in grain size are useful indicators of thermodynamic processes inside the snow pack. Changes in snow grain size can help in retrieving melt rates, an important parameter in snow melt runoff modeling and snowpack energy balance estimations.

The major scientific objective is to develop methods for retrieving snow pack characteristics in parts of Himalayan region. Detailed objectives are:

- To understand spectral characteristics of snow in different Himalayan environments.
- To develop techniques to retrieve the snow grain size and their rate of growth.
- To understand spatial and temporal variability of grain size at different latitude and altitudes.
- To develop techniques to estimate snow density
- To improve automated methods of snow type mapping
- To understand role of snow pack characteristics on albedo estimates
- To understand role of snow pack characteristics on snow melt estimates

#### **Study areas:**

Table 10: Study sites for snow and glacier studies

S.No.	Site	Longitude and Latitude		Remarks
1	Dhundi Himachal Pradesh	77.20	32.80	
		77.30	32.74	
		77.14	32.23	
		77.05	32.28	
2.	Patsio, Himachal Pradesh	77.20	32.76	Snow and Ice
		77.27	32.83	
		77.52	32.59	
		77.44	32.52	

#### **Approach**

- Derive the snow grain size from spectral data at different topographic regions and different seasons using inversion techniques
- Convert the grain size to snow density
- Assimilate snow density in distributed runoff model
- Estimate albedo from spectral data and use this data in radiative transfer model over Himalayan region.
- Carry out snow type mapping using improved NDSI methods.

**Methodology:** The major components of data analysis would include –

- Pre-processing of airborne imaging spectrometer data
- Radiometric correction of data using in-situ data & appropriate models
- Geo-referencing of multi-date data
- In-situ field data collection and database preparation
- Analysis for dimensionality reduction of imaging spectrometer data
- Determination of spectral signatures & indices
- Temporal pattern matching using imaging spectrometer signatures
- Modeling for Ice and snow properties assessment
- Validation.

AVIRIS data have been used to investigate the properties of snow and ice. Figure 15 shows one example for determining the melting status of snow based on the shift in the 1030 nm absorption band of ice towards the 980 nm absorption band of liquid water in a melting snow environment. As described above many other investigation of snow and ice properties are possible with AVIRIS measurements. In preparation for the airborne campaign, AVIRIS data sets from North America relevant to snow and ice in the Sierra Nevada mountains may be downloaded from the website [http://aviris.jpl.nasa.gov/alt\\_locator/](http://aviris.jpl.nasa.gov/alt_locator/) as calibrated radiance and atmospherically corrected reflectance. An additional snow and ice property being investigated inw the impact of dust on snow and related melting. Figure 16 shows an example AVIRIS data set collected follow a major dust deposition event in the mountains. This dust accelerates the melting of the snow and ice.



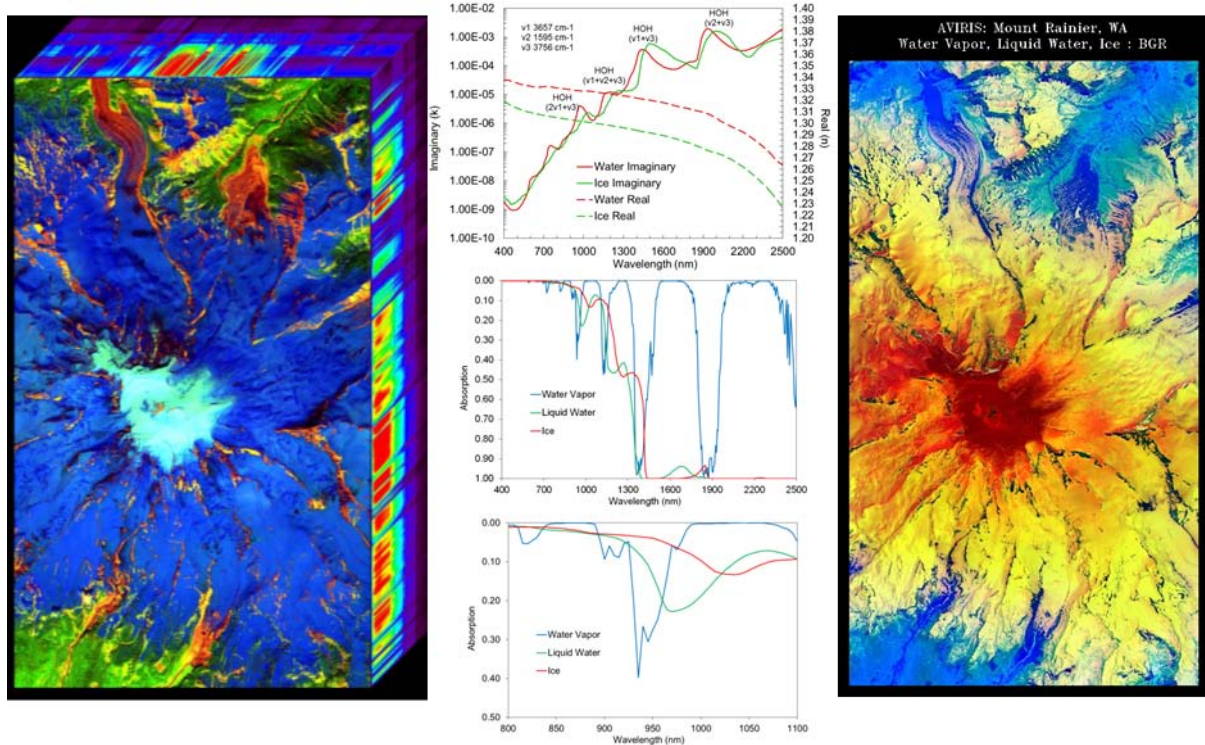


Figure 15. Example AVIRIS measurements over the snow and ice covered region of Mount Rainier, Washington. These measurements were used to determine the melting state of the snow by modeling the shift of ice absorption band near 1030 nm (R. Green).

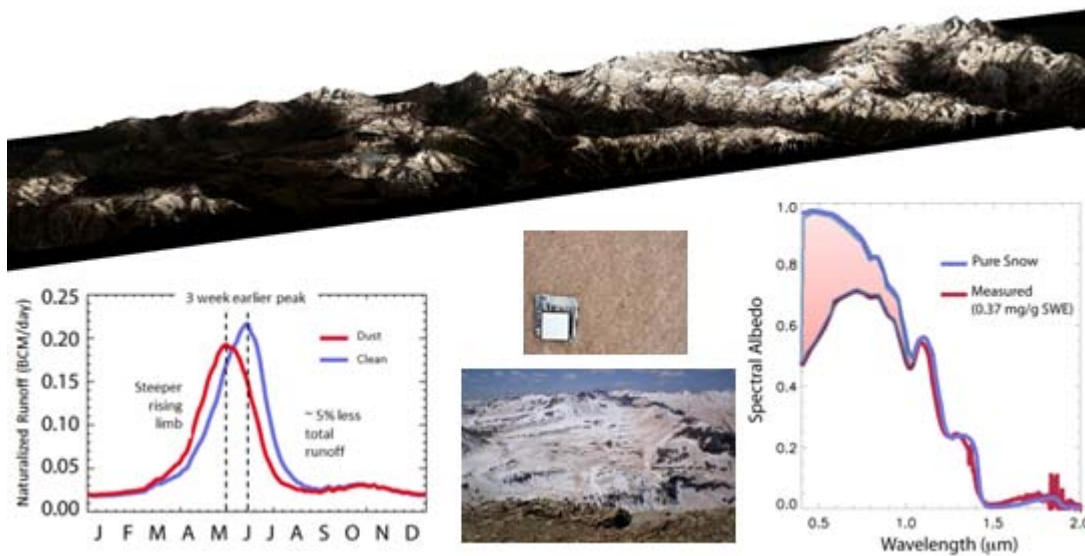


Figure 16. Example use AVIRIS measurement to measure the spectral albedo of snow and estimate the increased radiative forcing caused by dust. (T. Painter).

#### 4.6 URBAN AND CITIES

Urban areas are characterized by heterogeneous mix of materials such as cement concrete, steel, bituminous roads, G.I. sheets, tin, asbestos, stones, bricks, glass, wood, etc. The very

high resolution panchromatic and multi-spectral satellite images provide wealth of information on urban land cover composition largely in terms of Vegetation Impervious Soil (VIS) classification. VIS classification alone is not adequate for several studies such as urban hydrology, building stress, urban heat island characterisation etc. The spectral data provides information in terms of material composition of urban areas which the conventional multi-spectral images fail to detect.

The house-listing (H-series) census of India classifies the houses in terms of Material of Roof such as Grass/Thatch/Bamboo/Wood/Mud etc, Plastic/ Polythene, Handmade Tiles, Machine-made Tiles, Burnt Bricks, Stone/Slate, G.I./Metal/Asbestos sheets, Concrete, or any other material. Figure 17 shows the proportion of different types of roof materials in Census Houses as per Census of India 2011 in few Indian cities.

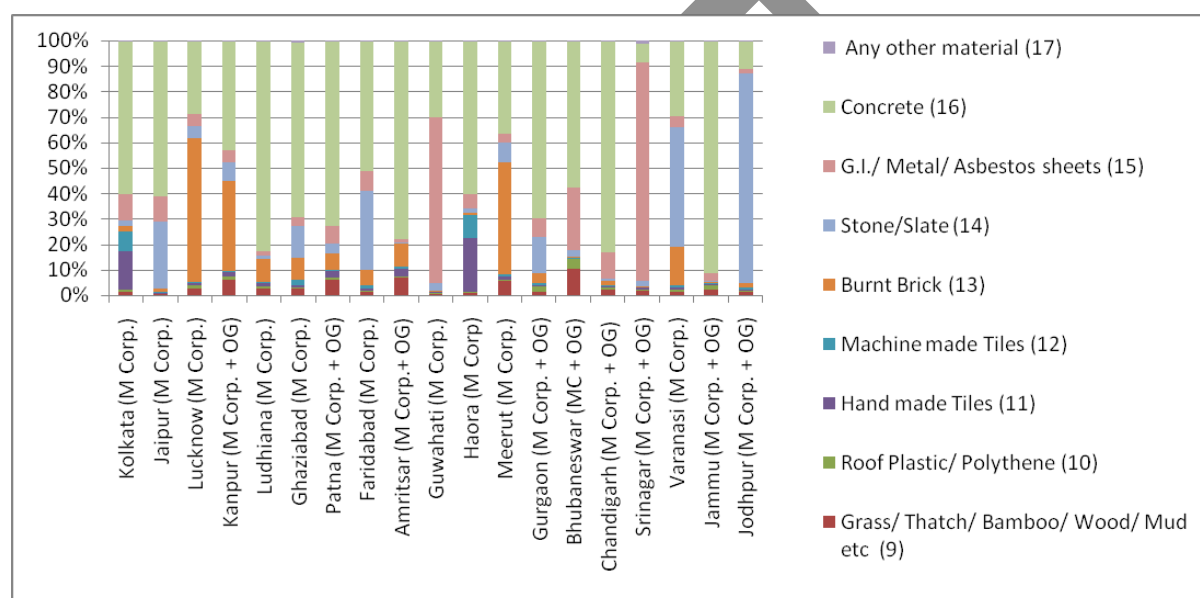


Figure 17 Material of roof of census houses in selected Indian cities (Census of India, 2011)

Again, the concrete roofs are often clad with multiple materials such as china-mosaic, tiles, paints, bituminous dam proofing courses, etc. Similarly, burnt brick and stone/ slate roofs may also be clad by other materials. This wide variety of materials as observed in the census H series tables can possibly be detected by spectral sensors.

The imaging spectrometer remote sensing has been demonstrated in several studies for improving urban land cover classification. Weng et al (2007) demonstrated application of EO-1 ALI imagery and Hyperion imagery in extraction of impervious surface in Indiana (USA). They identified impervious surfaces such as roads, building roofs, side walk and parking lots from the imaging spectrometer image with reasonable accuracy. Sugumaran et al (2007) attempted extraction of transportation infrastructure using 4.0 m, 380-2500 nm AVIRIS data in Shelton Nebraska and concluded that while quarry, highway, brick road, railroad, roof tops and fitness tracks can be separated with high accuracy, city streets and



concrete streets give low accuracy. Harold and Roberts (2010) successfully utilized high-resolution AVIRIS data in extracting red tile roofs, wood shingle roofs and asphalt roads. Figure 18 shows spectral profiles of typical land cover types and materials found in urban areas (Harold et al 2004). The study therefore attempts to study the spectral images on selected Indian cities characterised by widely varying roof-types and land cover types.

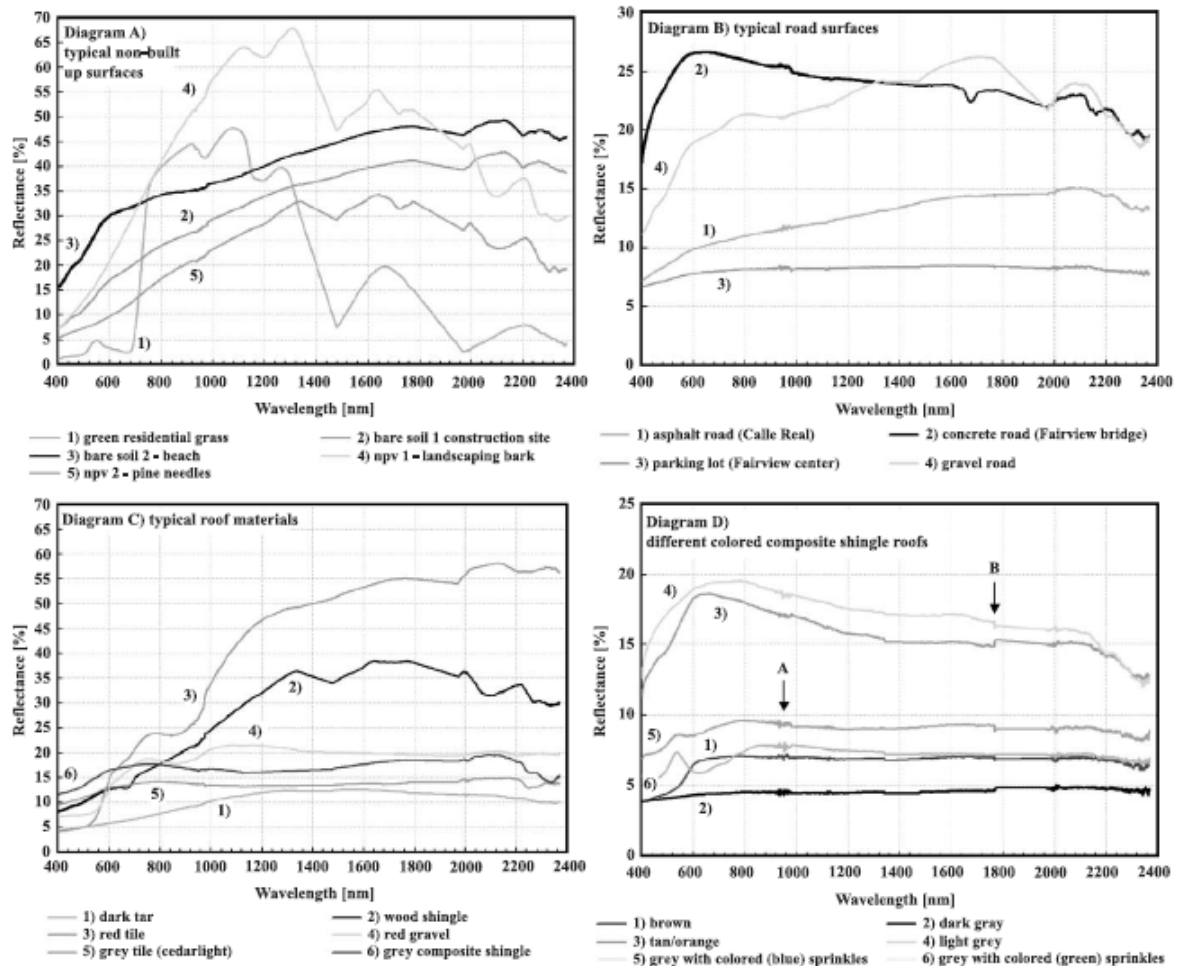


Figure 18 Spectra of typical land cover types and materials found in urban areas (harold et al 2004)

The main objectives of urban studies are given below:

- To characterize urban land cover material composition and building roof types using airborne spectral data. The roof-types classification on the basis of materials has significant potential in terms of assessment of impact of global warming on different urban roof materials.
- To characterize impervious/pervious land cover types in urban areas.: The spectral data holds potential in sub-classification of the pervious and impervious surfaces estimated within VIS land cover classification scheme which directly influences several applications such as storm water flow modeling, planning for low impact development

approaches such as bio-swales, bio-retention cells, permeable pavements etc, and urban heat island studies.

The study comprises of following cities selected on the basis of predominant composition of different building architectures/roof types in different geographic and climatic settings:

- **Ahmedabad city** covering part of inner city (densely populated old buildings), eastern Ahmedabad (predominance of industrial sheds), western Ahmedabad (relatively newer residential and commercial establishments), rural settlements and slums in semi-arid zone.
- **Jodhpur city** has due to its Arid climate has significant proportion of stone \ slate clad roofs. The city has 175,624 houses out of 212,898 census houses with stone clad roofs in arid zone.
- **Kalaburgi city** has significant proportion of houses with specially-made roofs.

Based on the feasibility, location for aerial survey would be decided. The map showing pervious/impervious land cover in urban area will be the key deliverable of the study. In addition to that map showing buildings with different materials of roofs in cities of different climatic zones will also be derived. The study will also identify slums and other areas of stressed housing conditions within the respective study area. The strategies on improving built-environment in cities of different types in order to mitigate global warming will be the final outcome of the study.

As described above, AVIRIS measurements have been used to study urban areas. These measurement have also been used to assess the impact of flood in New Orleans following a major storm. Figure 19 shows on of these AVIRIS data sets. AVIRIS data over the Los Angeles and San Francisco regions have also been measured. In preparation for the airborne campaign, AVIRIS data sets from North America relevant to urban environments may be downloaded from the website [http://aviris.jpl.nasa.gov/alt\\_locator/](http://aviris.jpl.nasa.gov/alt_locator/) as calibrated radiance and atmospherically corrected reflectance.

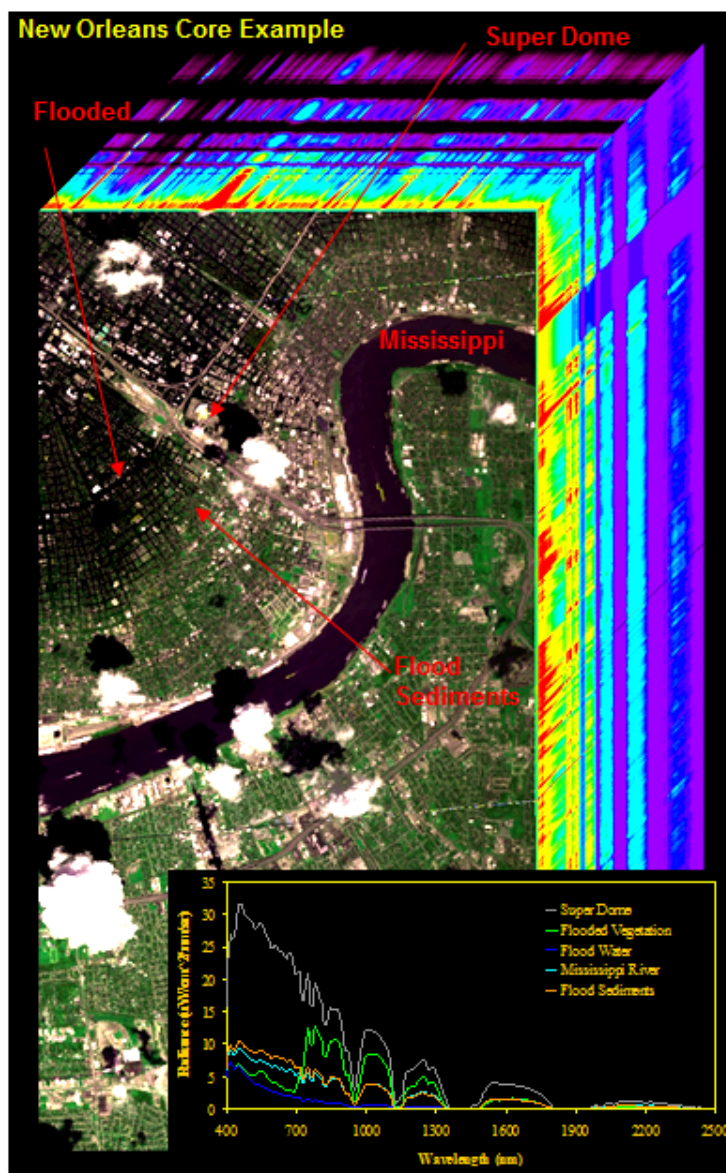


FIGURE 19. AVIRIS MEASUREMENT USED TO STUDY THE NEW ORLEANS URBAN AREA FOLLOWING A MAJOR FLOOD EVENT.

Table 11: Study sites for Urban studies

S.No.	Site	Longitude and Latitude	Remarks	Priority
1	Ahmedabad, Gujarat	78.16    32.80	Urban	1
		78.25    32.75		
		78.43    33.60		
		78.35    33.06		
2	Jodhpur, Rajasthan	72.87    26.19	Urban	2
		72.96    26.15		
		73.02    26.44		
		73.11    26.39		
6	Kalaburgi, Karnataka	76.94    17.36	Urban	1
		76.77    17.36		
		76.94    17.27		
		76.76    17.27		

## 4.7 COASTAL/OCEANOGRAPHIC APPLICATIONS

### A) BIOLOGICAL OCEANOGRAPHY

Coastal oceans encompass the coastal regions (river basins and estuaries) to seaward boundary of continental shelves. They are characterised by both case-1 and case-2 waters. Although the coastal oceans occupy only about 10% of the global ocean area, their proximity to land makes them susceptible to anthropogenic influences and climate change. Fluxes of material through major river systems to the coastal oceans are largely unidirectional from the land to the sea. Rates of primary production, export production, carbon flux to the sediments and burial in the coastal ocean are much higher than the open ocean. Intrinsic time and space scales of physical and biogeochemical variables are typically smaller in coastal domain and extremely dynamic in nature. Processes such as tides, topographic effects, shelf waves, coastal upwelling, jets meanders, fronts, internal waves, fresh water discharge and buoyancy driven flows characterise the physical domain of coastal oceans. Ecosystem complexity of coastal oceans is amplified by greater species diversity, a larger number of atmospheric and water pollutants and optically important constituents (coloured dissolved organic matter, suspended sediments and detrital matter). Occurrence of harmful algal blooms, nuisance blooms and invasive species are a matter of great concern to ecological managers and policy makers. Monitoring the coastal oceans require frequent sampling, higher spatial resolution sensors with additional spectral channels.

Imaging spectrometers give continuous spectral coverage over a broad wavelength range from near UV to near infrared with 5-10 nm spectral resolution. Such a sensor is ideally suited to study and characterise the optical and biological dynamics of coastal oceans. Several of the key structural and functional ecosystem variables are as yet poorly understood in coastal oceans surrounding the Indian subcontinent. Use of spectral imaging will greatly enhance the understanding of some of these ecosystem variables. The major objectives are listed below:

- Inherent optical properties (absorption, backscattering ) and composition ( chlorophyll  $-a$  , suspended sediments, CDOM) of coastal oceans
- Phytoplankton community structure through phytoplankton size classes and pigment composition
- Detection of harmful algal bloom, other blooms such as Trichodesmium
- Dissolved organic matter flux
- Identification of absorbing aerosols
- Phytoplankton physiology through chlorophyll fluorescence and absorption
- Bathymetry, bottom characterisation and benthic habitat mapping
- Bio-optical characterisation of Chilka lake

### *Selected Study Areas and Time for sampling*

- Coastal –offshore waters off Veraval and Porbandar region of Gujarat (January-March)
- Coastal –offshore waters off Goa (March-April)
- Coastal –offshore waters off Krishna-Godavari Basin (October-December)
- Chilka Lake (October-December)
- Coastal –offshore waters off Mangalore/Karwar (October-December, April- May)
- Lagoon area Off Bangaram, Agatti and Kavaratti (January -March)
- Figure 20 shows the biological coastal imaging sites planned for the mission.

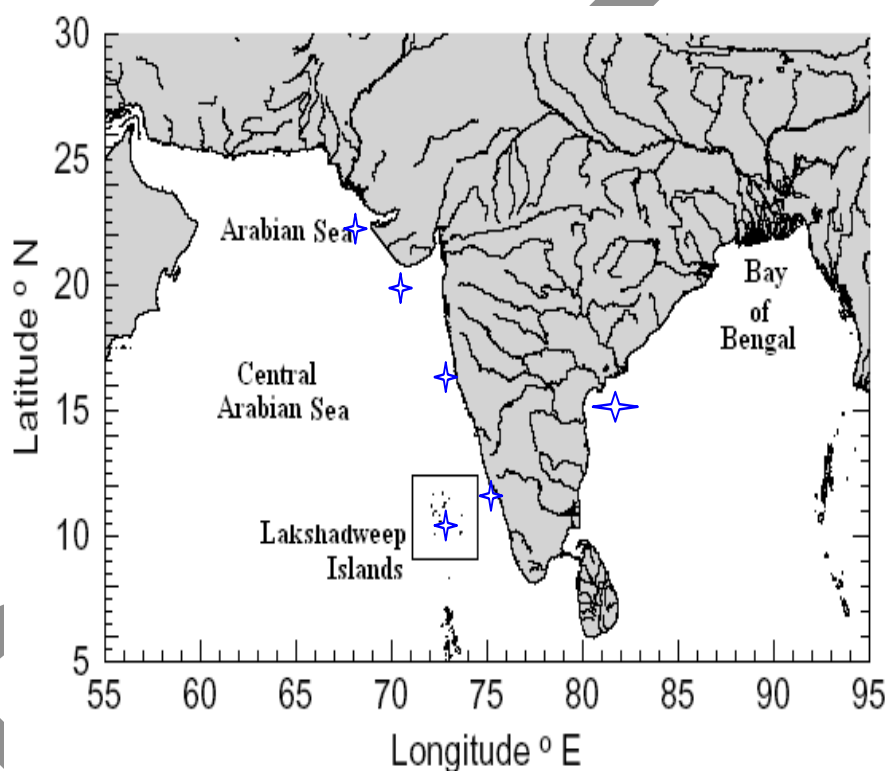


Figure 20 Sites for airborne sampling

The details are as mentioned below in Table 13:

Area	Coordinates		Priority
Coastal –offshore waters off Porbandar region of Gujarat	69.66	21.62	1
	69.32	21.45	
	69.24	21.51	
	69.57	21.68	
Coastal –offshore waters off Veraval region of Gujarat	70.45	20.87	1
	70.20	20.59	
	70.12	20.64	
	70.38	20.93	
Coastal –offshore waters off	73.93	15.31	1

Goa	73.56	15.25	
	73.54	15.34	
	73.90	15.39	
Coastal –offshore waters off Krishna-Godavari Basin	82.30	17.01	1
	82.61	16.88	
	82.21	16.35	
	82.05	16.41	
Chilka Lake	85.73	19.75	1
	85.78	19.66	
	85.18	19.34	
	85.14	19.41	
Coastal –offshore waters off Mangalore	74.88	12.82	1
	74.52	12.72	
	74.49	12.82	
	74.85	12.90	
Lagoon area Off Kavaratti	72.66	10.78	2
	72.75	10.75	
	72.59	10.33	
	72.51	10.36	
Lagoon area Off Bangaram, Agatti	72.28	11.03	2
	72.06	10.83	
	72.16	10.73	
	72.38	10.95	

## B) CRZ STUDIES

Discrimination and mapping of Ecological Sensitive Areas (Coastal land use/ land cover/landforms) are essential needs of –CRZ. Space Applications Centre is providing the CRZ maps for various users for their environmental clearance. These maps were prepared by LISS IV data of 2004-2006 time frame. LISS IV data is having only 4 spectral bands in VIR region. Though it is useful in delineation of various coastal features, it has wide spectral bands and confine to NIR which limit the classification accuracy beyond certain level. In order to meet the requirements of CRZ Notification, 2011, it is essential to improve the existing classification accuracy and improving classification system up to level IV. It is proposed to utilize spectral data for this purpose.

### Objectives

The major objective is to spectrally discriminate various coastal landuse/land cover and landform classes and improve the classification accuracy of CRZ maps.

The detailed objectives are:

- Understanding spectral signatures of various coastal land cover and landform classes
- Understanding spectral signatures of various nearshore water quality parameters such as pollutants/sewage/oil slicks etc. within CRZ classes as per 2011 Notification.
- Improving discrimination and classification accuracy of above mentioned features related to CRZ.
- Improving HTL/LTL discrimination

### Study Area:

- Gulf of Kachchh in Gujarat
- Chilika lagoon and environs, Odisha
- Coringa creek, Kakinada coast of Andhra Pradesh
- Selected Coastal Metropolitan cities Mumbai./Chennai
- South Karnataka coast around Mangalore region
- Parts of Lakshadweep and A&N islands

The details are mentioned in Table 14 below:

Area	Long, Lat		Priority
Gulf of Kutch, Gujarat	69.3	22.29	1
	69.75	22.44	
	69.66	22.72	
	69.3	22.29	
	69.75	22.44	
	69.66	22.72	
	69.3	22.29	
	69.75	22.44	
	69.66	22.72	
	69.3	22.29	
	69.75	22.44	
	69.66	22.72	
	69.66	22.82	
69.65	22.73		
Chilika lagoon and environs, Odisha	85.03	19.57	1
	84.98	19.65	
	85.59	19.99	
	85.63	19.91	
	85.08	19.49	
	85.03	19.57	
	85.64	19.91	
	85.68	19.83	
	85.13	19.41	
	85.08	19.49	



	85.69	19.83	
	85.73	19.75	
Selected Coastal Metropolitan cities Mumbai	72.92	18.76	2
	72.82	18.75	
	72.71	19.25	
	72.81	19.26	
	73.01	18.78	
	72.92	18.76	
	72.81	19.26	
	72.90	19.27	
	73.11	18.79	
	73.01	18.78	
	72.90	19.27	
	73.00	19.29	
South Karnataka coast around Mangalore region	74.71	13.24	1
	74.80	13.26	
	74.91	12.82	
	74.82	12.80	
Parts of Lakshadweep islands	72.66	10.78	2
	72.75	10.75	
	72.59	10.33	
	72.51	10.36	

#### Expected end results:

- Discrimination of level IV classes of CRZ Maps
- Improved classification accuracy of coastal landuse/ land cover/landforms
- Discrimination of coastal pollutants and development of digital methods for nearshore water quality parameters.

In addition to the benthic substrate, AVIRIS has been used for the investigation of in water planktonic species detection and measurement. Figure 21 shows an AVIRIS data mosaic and extracted spectra from areas with and without a phytoplankton bloom. The spectral signature measure by AVIRIS enables extraction of a range of in water physical and biological properties. In preparation for the airborne campaign, AVIRIS data sets from North America relevant coastal and offshore environments may be downloaded from the website [http://aviris.jpl.nasa.gov/alt\\_locator/](http://aviris.jpl.nasa.gov/alt_locator/) as calibrated radiance and atmospherically corrected reflectance.

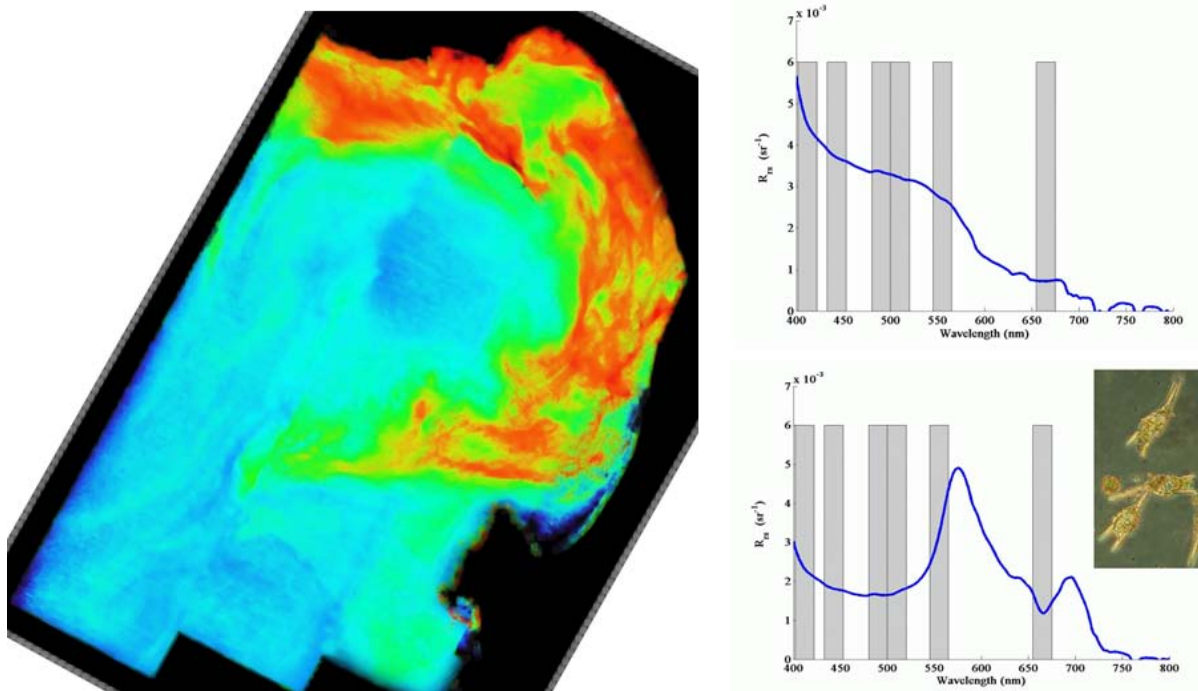


**Figure 21. Example AVIRIS data set mosaic collected over Monterey Bay, California during a phytoplankton bloom. A wide diversity of biological and physical oceanographic phenomena are recorded in the AVIRIS spectral signatures.**

#### 4.8 CLOUD AND ATMOSPHERE

The temporal monitoring of cloud microphysics is of extreme importance in forecasting the precipitation development processes. Also the long-term changes in the cloud structural properties can affect the global radiation budget. Thus observation of cloud properties like effective radius, thermodynamic phase, optical depth is crucial not only for short term weather forecasting but also for climate scale studies. According to the study by Meenu et al., (2010), Bay of Bengal (BoB) and the east equatorial Indian Ocean are among the most intense deep convective regions over the tropics, with frequency of occurrence peaking at 16.5 Kms. Figure 22 gives monthly mean spatial distribution of the high altitude cloud fraction (in percentage).

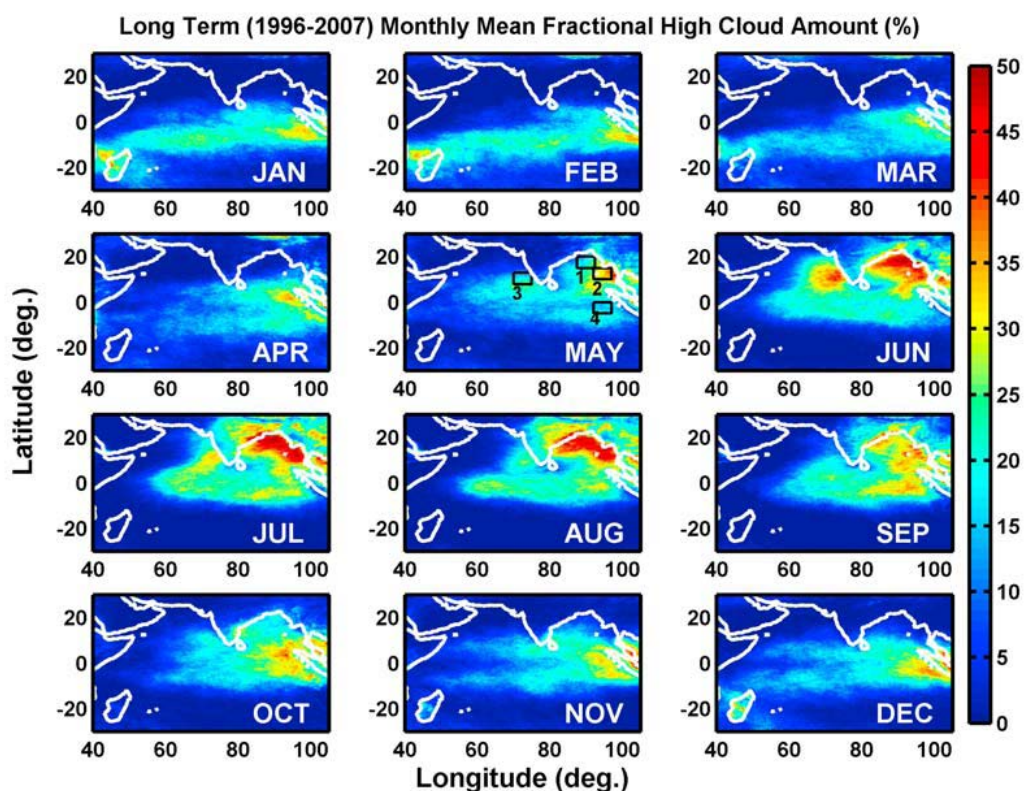


Figure 22 As adapted from Meenu et al., (2010)

Similarly the retrieval of surface pressure from satellite based observations is extremely useful for filling the gaps of surface based measurements. However, it is a very ambitious task due to the precision required for its derivation (Lindstrot et al., 2010). Airborne spectral measurements provide an opportunity to develop and validate methodology for the same. The major objectives are to derive atmospheric parameters:

- Cloud microphysical parameters
- Water vapour concentration
- Surface/ cloud top pressure derived from O<sub>2</sub> absorption band

A summary of the desired atmospheric parameters, spectral wavelengths and location of interest is provided in the Table 10 below:

Table 15. Study area atmosphere correction experiment

S.No	Atmospheric parameters	Wavelength (mm) sensitive to atmospheric parameters	Desirable Geographical coverage (Long, lat)
1	Cloud effective radius	2.1	Mangalore East-West, Karnataka
2	Cloud Optical Depth		73.85 12.88
	Over land	0.6	74.85 12.88

	Over ocean	0.8	74.85	12.83
	Over snow & sea ice surfaces	1.2	73.85	12.83
3	Thermodynamic Phase	1.6	Mangalore	North-South, Karnataka
4	Liquid water path	Derived Product	74.80	12.88
5	Ice Water Path	Derived Product	74.85	12.88
			74.85	11.88
6	Contrail detection	1.88	74.80	11.88
			(above cloud upto a height of 17 kms)	
7	Water Vapour concentration	0.72,1.87,2.7	-	
8	Surface pressure derived from Oxygen A Band	0.76	Near	ground observation sites of Cochin, Kolkata

The retrieval of cloud microphysical parameters will be based on radiative transfer modeling and inversion, preferably by a look-up-table approach. The derivation of surface pressure will be carried out through a differential absorption technique.

In addition to the investigations described above AVIRIS measurement has been used to separate liquid water clouds from ice clouds. Figure 23 show mapping of liquid water and ice clouds and the corresponding spectroscopic fitting methods. In preparation for the airborne campaign, AVIRIS data sets from North America relevant to the study of cloud and atmospheric properties may be downloaded from the website [http://aviris.jpl.nasa.gov/alt\\_locator/](http://aviris.jpl.nasa.gov/alt_locator/) as calibrated radiance.



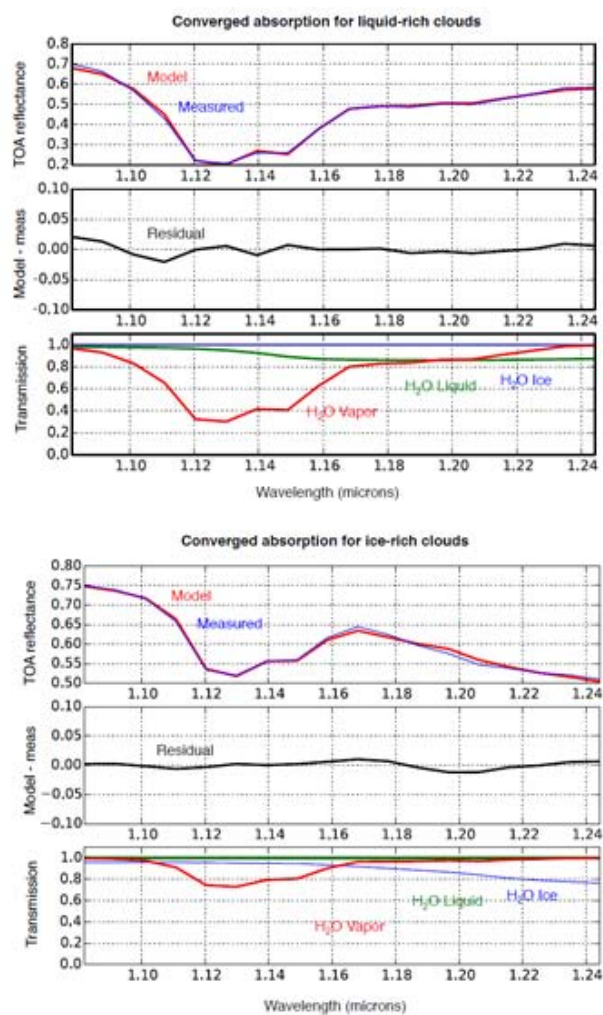
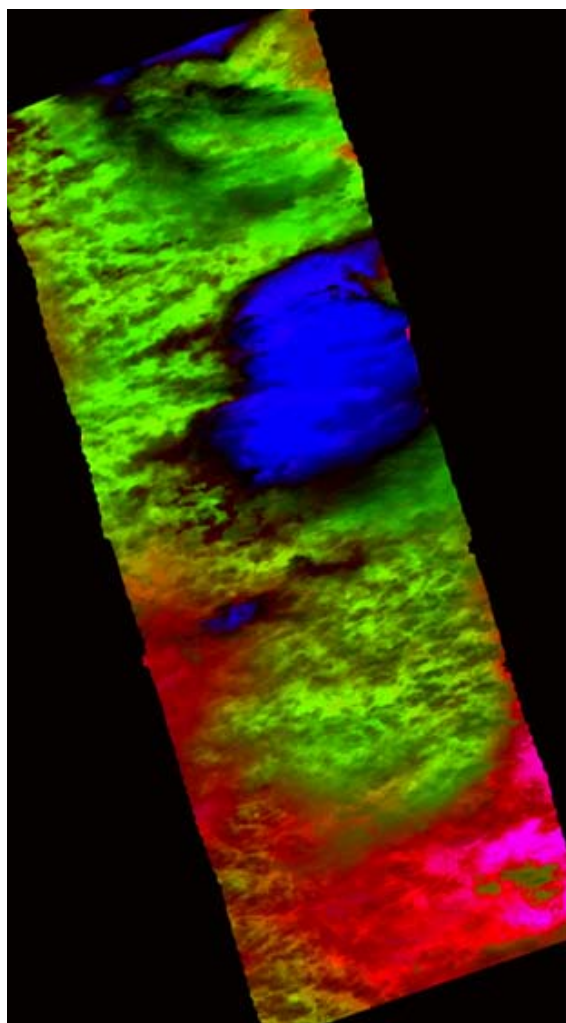


Figure 23. Example showing the separation liquid water clouds from ice clouds with spectroscopic measurements by AVIRIS.

## 5.0 CALIBRATION OF AIRCRAFT AND SATELLITE SENSORS

Since the early 1990s, the availability of remote sensing imagery in the solar reflective spectrum (400 to 2500nm) has seen advancement. The airborne and space sensors cover variety of spatial and spectral (from multi-spectral to fully spectral) resolutions. The critical component of use of such data from these systems depends on sensor definition, pre-flight and in-flight radiometric calibration. Radiometric calibration is the first step in any remote-sensing application. It is also the precondition for the synergy of multisource data assimilation. In-flight calibration methods rely on in-situ measurements of the ground reflectance and atmospheric parameters.

Although the radiometric calibration of space payloads (OCM2, AWiFS, and Insat-3D) has been developed at Kavaratti, little Rann of Kutch and greater Rann of Kutch sites, the present attempt will yield the in-flight calibration of airborne payload. The vicarious calibration of airborne sensor has challenge in modelling the radiative transfer code below the layer of 2Km where at atmosphere is heterogeneous while compare to the satellite sensor altitude.

An hybrid approach of reflectance based method along with spectra measured with the ASD (Analytical Spectral Device) field spectrometer, radiative transfer model will be used to simulate radiance and reflectance spectra at aircraft level for multiple theoretical geometry (the uncertainty of the reflectance based methods can reach upto 2.5%). The main restriction with the reflectance-based method is the state of the atmosphere. It requires knowledge about the atmospheric transmission, the vertical column profiles of water vapor, pressure, temperature, the total column ozone, and aerosol asymmetry as well as the size distribution.

During our field campaign (areal survey) ASD, CIMEL sun photometer, MicroTop-II sun photometer and ozonometer will be used for the modeling purpose. This acquired low-altitude spectral data sets along with other mentioned ancillary measurement will be used to produce benchmark data sets in the spectral bands and thus will be used to define the future space borne spectral instruments. Below 24 shows some of the bench mark reflectance spectrum.

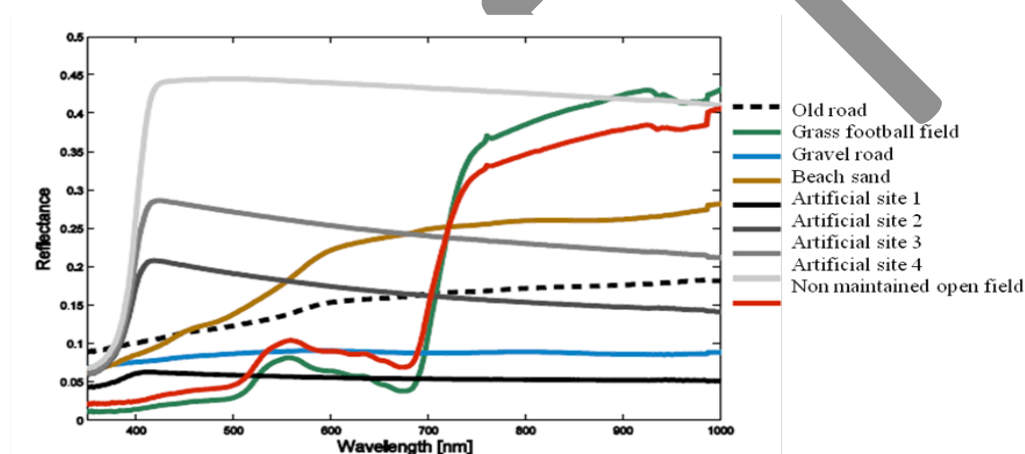


Figure 24 Example OF THE NADIR FIELD REFLECTANCE SPECTRA (CURTSEY - LAURI MARKELIN; [HTTP://URN.FI/URN:ISBN:978-951-711-295-6](http://urn.fi/URN:ISBN:978-951-711-295-6)).

Study area:

**(1) NRSC Shadnagar, Hyderabad:**

Strip region: 78.182 to 78.185 E, 17.032 to 17.035 N

**(2). Desalpar site:**

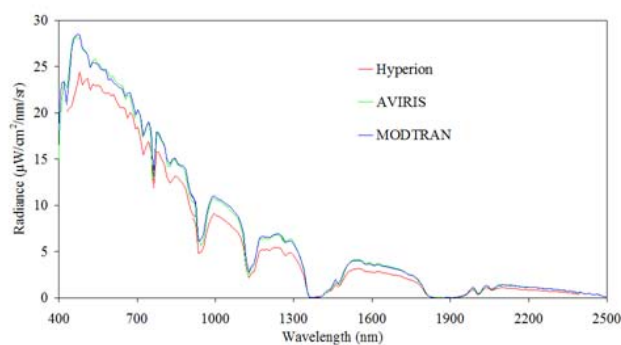
Exact location: 70.69E; 23.79N

Strip region: 70.45E to 70.95E; 23.78N to 23.83N

Outcome: Post launch vicarious calibration gain and periodic updates on sensor performance over bright and dark reflectance targets.

In the past AVIRIS measurements have been used to validation and update the on-orbit radiometric calibration of Earth observing satellite system. Figure 25 shows the data set collected in 2001 for the on-orbit calibration and validation of the Hyperion imaging spectrometer. AVIRIS measurements can be convolved to the spectral bands of multi-spectral systems for calibration and validation objectives. AVIRIS has under flown Landsat for calibration purposed on a number of occasions. In preparation for the airborne campaign, AVIRIS data sets from North America collected over large homogeneous dry lake surface may be downloaded from the website [http://aviris.jpl.nasa.gov/alt\\_locator/](http://aviris.jpl.nasa.gov/alt_locator/) as calibrated radiance.

## Hyperion



## AVIRIS

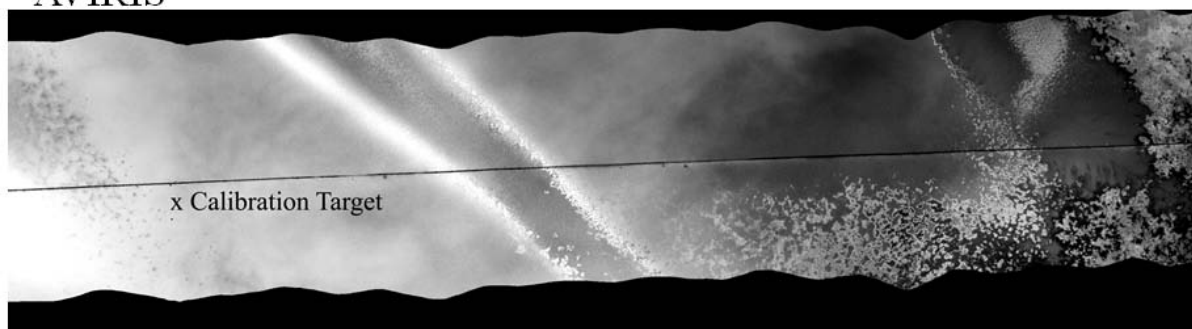


Figure 25. Example use of AVIRIS for the on-orbit validation and calibration update of the Hyperion imaging spectrometer in 2001.

## References

Anger, C.D., Babey, S.K., and Adamson, R.J., 1990. A new approach to imaging spectroscopy. Proc. SPIE Conference on Imaging Spectrometry of Terrestrial Environment, Orlando, Florida, Vol. 1298, pp. 72-86.

AVIRIS, 2007. AVIRIS Workshop Bibliographies. <http://aviris.jpl.nasa.gov/html/aviris.biblios.html> (accessed April 20, 2009).

Barnsley, M.J., Settle, J.J., Cutter, M.A., Lobb, D.R., and Teston, F., 2004. The PROBA/CHRIS mission: a low cost smallsat for hyperspectral multiangle observations of the earth surface and atmosphere. IEEE Trans. Geosci. Remote Sens., 42(7), pp. 1512-1519.



Bezy, J-L., Delwart, S., and Rast, M., 2000. MERIS-A new generation of ocean-colour sensor onboard Envisat. *ESA Bulletin*, Vol. 103, pp. 48-56.

Bhattacharya, B. K. and Chattopadhyay, C., 2013. A multi-stage tracking for mustard rot disease combining surface meteorology and satellite remote sensing. *Computers and Electronics in Agriculture*, 90, 35 – 44.

Bhattacharya, S., Majumdar, T.J., Rajawat, A.S., Panigrahy, M.K., Das, P.R., 2012. Utilization of Hyperion data over Dongargarh, India, for mapping altered/weathered and clay minerals along with field spectral measurements. *International Journal of Remote Sensing*, 33(17), 5438–5450.

Birk, R.J., and McCord, T.B., 1994. Airborne hyperspectral sensor systems. *IEEE Aerospace and Electronic Systems Magazine*, 9(10), pp. 26-33.

Boardman, J.W., 1993. Automating spectra unmixing of AVIRIS data using convex geometry concepts. *Summaries of the 4th Annual JPL Airborne Geoscience Workshop*, JPL Publication 93-26, Pasadena, California, Vol. 1, pp. 11-14.

Boardman, J.W., Biehl, L.L., Clark, N.N., Kruse, F.A., Mazer, A.S., Torson, J., and Staenz, K., 2006. Development and implementation of software systems for imaging spectroscopy. *Proc. Int. Geosci. Remote Sens. Symp. (IGARSS'06)*, Denver, Colorado, pp. 1969-1973.

Buckingham, R., and Staenz, K., 2008. Review of current and planned civilian space hyperspectral sensors for EO. *Can. J. Remote Sens.*, 34(Supplement 1), pp. S187-S197.

Camps-Valls, G., Gomez-Chova, L., Calpe-Maravilla, J., Martin-Guerrero, J.D., Soria-Olivas, E., Alonso-Chorda, L., and Moreno, J., 2004. Robust support vector method for hyperspectral data classification and knowledge discovery. *IEEE Trans. Geosci. Remote Sens.*, 42(7), pp. 1530-1542.

Das, B. S., Sarathjith, M. C., Santra, P., Sahoo, R. N., Srivastava, R., Routray, A., Ray, S. S., 2015. Hyperspectral remote sensing: opportunities, status and challenges for rapid soil assessment in India. *Current Sci.*, 108(5), 860-868.

Dutta, S., Bhattacharya, B. K., Rajak, D. R., Chattopadhyay, C., Patel, N.K. and Parihar, J.S., 2006. Disease detection in mustard crop using EO-1 Hyperion satellite data. *Journal of the Indian Society of Remote Sensing*, 34(3), 311 – 316.

Galeazzi, C., Varacalli, G., Longo, F., Lopinto, E., Garramone, L., and Capentiero, R., 2009. Overview of the PRISMA mission. *Proc. 6th EARSel SIG Workshop on Imaging Spectroscopy*, Tel Aviv, Israel (in this proceedings).

Goetz, A.F.H., 2009. Three decades of hyperspectral remote sensing of the Earth: A personal view. *Remote Sens. Environ.*, doi: 10.1016/j.res.2007.12.014.

Gower, J.F.R., Borstad, G.A., Gray, L.H., and Edrel, H.R., 1987. The Fluorescence Line Imager: Imaging spectroscopy over water and land. *Proc. 11th Can. Symp. on Remote Sens.*, Waterloo, Ontario, pp. 689-697.

Green, R.O., Asner, G., Ungar, S., and Knox, R., 2008. NASA mission to measure global plant physiology and functional types. *Proc. IEEE Aerospace Conference, Big Sky, Montana*, pp. 1-7.

Khurshid, S., Staenz, K., Sun, L., Neville, R.A., White, H.P., Bannari, A., Champagne, C.M., and Hitchcock, R., 2006, Preprocessing of EO-1 Hyperion data. *Can. J. Remote Sens.*, 32(3), pp. 84-97.

Neville, R.A., Sun, L., and Staenz, K., 2008. Spectral calibration of imaging spectrometers by atmospheric absorption feature matching. *Can. J. Remote Sens.*, 34(Supplement 1), pp. S29-S42.

Pearlman, J.S., Barry, P.S., Segal, C.C., Shepanski, J., Beiro, D., and Carman, S.L., 2003. Hyperion a space based imaging spectrometer. *IEEE Trans. Geosci. Remote Sens.*, 41(6), pp. 1160-1173.

Ramakrishnan, D. and Bharti, R., 2015. Hyperspectral remote sensing and geological applications. *Current Sci.*, 108(5), 879-891

Rivard, B., Feng, J., Gallie, A., and Sanchez-Azofeifa, A., 2008. Continuous wavelets for the improved use of spectral libraries and hyperspectral data. *Remote Sens. Environ.*, 112, pp. 2850-2862.

Sahoo, R. N., Ray, S. S., Manjunath, K. R., 2015. Hyperspectral remote sensing of agriculture. *Current Sci.*, 108(5), 848-859.

Schaepman, M.E., Ustin, S.L., Plaza, A.J., Painter, T.H., Verrelst, J., and Liang, S., 2009. Earth system science related imaging spectroscopy – An assessment. *Remote Sens. Environ.*, doi: 10.1016/j.res.2009.03.001.

Staenz, K., and William, D.J., 1997. Retrieval of surface reflectance from hyperspectral data using a look-up table approach. *Can. J. Remote Sens.*, 23(4), pp. 354-368.

Staenz, K., Schwarz, J., Vachon, F., and Nadeau, C., 1999. Classification of hyperspectral agricultural data with spectral matching techniques. *Proc. Int. Symp. on Spectral Sensing Research*, Las Vegas, Nevada, U.S.A., CD-ROM (8 pages).

Staenz, K., 2009. Terrestrial imaging spectroscopy – some future perspectives. Personal Communication.

Stuffer, T., Kaufmann, H., Hofer, S., Forster, K.-P., Schreier, G., Muller, A., Eckardt, A., Bach, H., Penne, B., and Haydn, R., 2007. The EnMAP hyperspectral imager - An advanced optical payload for future applications in Earth observation programmes. *Acta Astronautica*, 61(1-6), pp. 115-120.

Takahashi, D., 2009. The world's first commercial hyperspectral data service from Japanese ALOS-3 satellite. <http://www.isiswg.org/documents/Hyper-X%20v%204%204%20090302.pdf> (accessed May 11, 2009).

Van Aardt, J.A.N., and Coppin, P.R., 2006. Current state and potential of the IS-HIS Project – Integration of *in situ* data and hyperspectral remote sensing for plant production modeling. *Proc. IUFRO International Precision Forestry Symp.*, Stellenbosch, South Africa, pp. 33-42.

Vane, G., and Goetz, A.F.H., 1988. Terrestrial imaging spectroscopy. *Remote Sens. Environ.*, 21(1), pp. 1-29.

Vane, G., Green, R.O., Chrien, T.G., Enmark, H.T., Hansen, E.G., and Porter, W.M., 1993. The Airborne Visible/Infrared Imaging Spectrometer (AVIRIS). *Remote Sens. Environ.*, 44, pp. 127-143.

Ward, S., and Berger, M., 2007. ESA's activities supporting hyperspectral remote sensing. [http://www.isiswg.org/meetings/isiswg1/materials/ISIS\\_WS\\_Hawaii\\_2007ppt.pdf](http://www.isiswg.org/meetings/isiswg1/materials/ISIS_WS_Hawaii_2007ppt.pdf) (accessed April 20, 2009).

Zarco-Tejada, P. J., Miller, J.R., Noland, T.L., Mohammed, G.H., and Sampson, P.H., 2001. Scaling-up and model inversion methods with narrow-band optical indices for chlorophyll content estimation in closed forest canopies with hyperspectral data. *IEEE Trans. Geosci. Remote Sens.*, 39: 1491–1507.

Zhang, J., Staenz, K., Rochdi, N., Teillet, P.M., Ren, X., Lowe, D., and Eddy, P., 2009. Automatic surface reflectance retrieval from SPOT data using a MODTRAN-based look-up table. *Proc. Can. Symp. on Remote Sens.*, Lethbridge, Alberta.